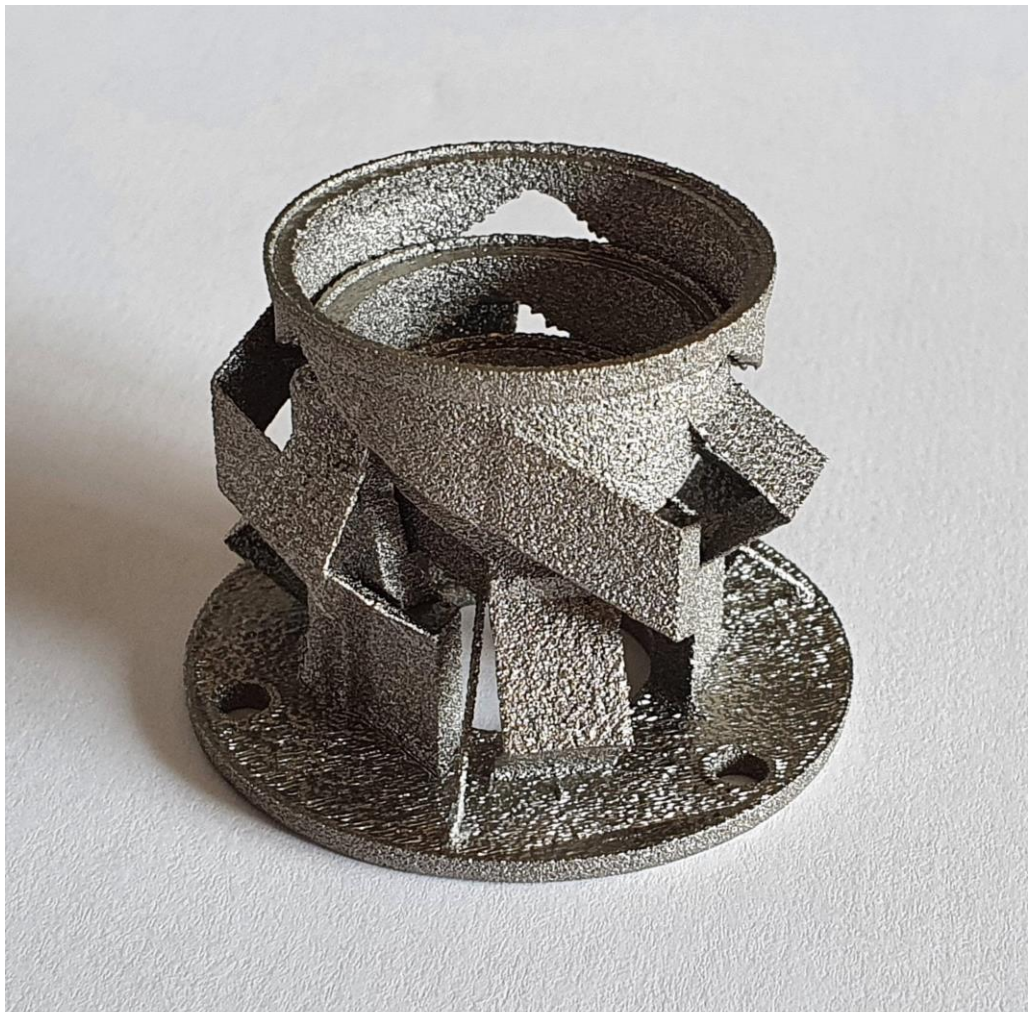


Department of Precision and Microsystems Engineering

Design method for 3D printed compliant mechanisms

T.R. Oude Vrielink

Report no : 2021.079
Coach : Dr. ir. L.A. Cacace
Professor : Prof. dr. ir. J.L. Herder
Specialisation : MOOM
Type of report : Thesis
Date : 15 October 2021



Design method for 3D printed compliant mechanisms

by

T.R. Oude Vrielink

to obtain the degree of Master of Science
at the Delft University of Technology,
to be defended publicly on Thursday Oktober 29, 2021 at 10:30 AM.

Student number:	4285956
Project duration:	october 2020 – october 2021
Thesis committee:	Prof. dr. ir. J.L. Herder, TU Delft, chair
	Dr. ir. L. A. Cacace, TU Delft, supervisor
	Dr. ir. J. de Vreugd, TNO
	Dr. ir. W. J. Westerveld, TU Delft

An electronic version of this thesis is available at <http://repository.tudelft.nl/>.

Summary

Optical components are used in many different applications such as satellite imaging, scientific instruments, industrial manufacturing and medical applications. Because the wavelength of light is in the sub-micrometer range, some of the tolerances on high performance optical systems are in the micro- to nanometer range. To reach the desired performance in these systems, the optical components have to be placed within these tolerances and alignment is one of the methods of achieving this.

Multi-body mechanisms consisting of conventional hinges and couplings have many applications in which they are very useful but have some distinct disadvantages when applied in high precision systems. The assembling of multiple parts can introduce lower overall stiffness in the mechanism, friction in moving parts, mismatched thermal properties, thermal barriers, stacking of tolerances and extra costs. Compliant mechanisms provide a solution to these issues. Compliant mechanisms function through the elastic deformation of flexures which are compliant in some directions and stiff in others. Everything but the desired direction of movement can be constrained by arranging these flexures in a specific manner. Because movement is achieved through elastic deformation, compliant mechanisms can be made as monolithic parts. This enables them to be predictable and operate without friction or play.

Compliant mechanisms are usually made with conventional manufacturing techniques such as milling and spark erosion. These methods have limitations which make some geometries considerably expensive or impossible to manufacture. Metal 3D printing is a newer manufacturing method with unique capabilities and limitations. It can produce monolithic parts with great geometrical freedom but is limited in what it can achieve in some aspects. The layer by layer process, the powder feed stock and the use of high power lasers all introduce design constraints. The compliant mechanisms that can be produced with conventional methods are well documented and known. This is not yet the case for metal 3D printing. The solution space is defined by new rules, is quite large and not fully explored. These factors present obstacles for designers in making effective use of metal 3D printing for the production of alignment mechanisms.

This study aims at developing a design method to help designers use the large solution space of metal 3D printing to create compliant alignment mechanisms. The overarching goal is to develop a design method with building blocks, guidelines and strategies to solve problems related to compliant alignment mechanisms for metal 3D printing. This thesis is intended to make a start towards achieving this goal. This start consists of a set of printable building blocks, a system to order these elements and a method to use them to develop concepts for compliant 3D printed alignment mechanisms.

A method of structuring building blocks is presented followed by the tools needed to construct building blocks and the building blocks themselves. These are then presented in three complementary tables. A flowchart is used to describe a design method for applying the tables and building blocks towards the development of concepts for metal 3D printed compliant alignment mechanisms. The design method is then applied to an example case. The example is developed by stating design requirements, developing concepts using the design method and integrating them into a conceptual design that complies with the design requirements. This conceptual design serves as a starting point for optimization or creative design alterations. Some of the properties of the conceptual mechanism are explored using finite element analysis and a prototype manufactured in Ti6Al4V. The thesis is concluded with a discussion on using the design method and a set of recommendations for future research.

*T.R. Oude Vrielink
Delft, Oktober 2021*

Acknowledgements

I would like to thank all those who helped and supported me during this past year and made this thesis possible. I would like to thank my mentor dr. ir. Lennino Cacace for all the advice and guidance he has given me in my work on this thesis and on engineering in general. I've learned a lot from you. I would like to thank TNO and my supervisor dr. ir. Jan de Vreugd for their support during the orientation phase of this research and making it possible to create a prototype. To my fellow students, thank you for providing feedback during our OM-meetings. Especially during this past year, where distance to and contact with peers has decreased so much. And finally I would like to thank my wife Daphne for her motivating words, patience and listening to my endless stories about 3D printing and flexures. You've made this past year the happiest one I've experienced yet.

*T.R. Oude Vrielink
Delft, Oktober 2021*

Contents

1	Introduction	1
1.1	3D printing for OM	1
1.2	Compliant mechanisms	1
1.3	Influence of manufacturing technologies	2
1.3.1	Machining	2
1.3.2	Spark erosion	3
1.3.3	Metal 3D printing	3
1.4	Research goal	6
1.5	Approach and structure	6
1.6	Definitions	7
	Start of paper	9
1	Introduction	10
1.1	3D printing for OM	10
1.2	Research goal	11
1.3	Approach and structure	11
1.4	Definitions	11
2	Building blocks	11
2.1	Structuring approach	11
2.2	Constraint representation by strut configurations	12
2.3	Substitution elements	12
2.4	Printable building blocks	13
2.5	Design method	13
3	Demonstration casse	19
3.1	Design goals	19
3.2	Tip/tilt concept selection	19
3.3	Focus concept selection	19
3.4	Center concept selection	20
3.5	Integrating designs	21
4	Analysis	22
4.1	Methods	22
4.2	Characterizing alignment stages	22
4.3	Exploring improvements	23
4.4	Prototype	25
5	Conclusion	25
6	Recommendations	25
	References	27
	End of paper	28
7	Conclusion and recommendations	29
7.1	Conclusion	29
7.2	Recommendations	30
A	Appendix	33
	Bibliography	41

1

Introduction

1.1. 3D printing for OM

Optical components are used in many different applications such as satellite imaging, scientific instruments, industrial manufacturing and medical applications. Because the wavelength of light is in the sub-micrometer range, some of the tolerances on high performance optical systems are in the micro- to nanometer range. To reach the desired performance in these systems, the optical components have to be placed within these tolerances and alignment is one of the methods of achieving this. Multi-body mechanisms consisting of conventional hinges and couplings have many applications in which they are very useful but have some distinct disadvantages when applied in high precision systems. The assembling of multiple parts can introduce lower overall stiffness in the mechanism, friction in moving parts, mismatched thermal properties, thermal barriers, stacking of tolerances and extra costs. Compliant mechanisms provide a solution to these issues [9], [11]. Compliant mechanisms function through the elastic deformation of flexures which are compliant in some directions and stiff in others. Everything but the desired direction of movement can be constrained by arranging these flexures in a specific manner. Because movement is achieved through elastic deformation, compliant mechanisms can be made as monolithic parts. This enables them to be predictable and operate without friction or play. Compliant mechanisms are usually made with conventional manufacturing techniques such as milling and spark erosion. These methods have limitations which makes some geometries considerably expensive or impossible to manufacture. Splitting a monolithic design into multiple parts can be the only way to manufacture it with conventional techniques in some situations. Metal 3D printing is a newer manufacturing method with unique capabilities and limitations. The process considered in this thesis is selective laser melting (SLM). It can produce monolithic parts with great geometrical freedom but is limited in what it can achieve in some aspects. The layer by layer process, the powder feed stock and the use of high power lasers all introduce design constraints [6]. The main limitation with metal 3D printing processes is the limited capability to manufacture overhanging geometries. The critical overhang angle is between 60° and 30° , defined as angle α in figure 1.1, depending on the particular machine and material. When geometries are below this self-supporting angle, fabricating defects occur. Titanium alloys generally allow for lower overhang angles [1], are suitable for creating flexures due to their ratio between yield strength and young's modulus [8], [2], and are compatible in thermal expansion coefficient with many glass types [3], [10]. The compliant mechanisms that can be produced with conventional methods are well documented and known. This is not yet the case for metal 3D printing. The solution space is defined by new rules, is quite large and not fully explored. These factors present obstacles for designers in making effective use of metal 3D printing for the production of alignment mechanisms.

1.2. Compliant mechanisms

Conventional mechanisms consist of rigid bodies that are connected to each other with various hinge types. These hinges also consist of one or more separate rigid bodies. Conventional mechanisms can be simpler to understand, design, manufacture and maintain as the functions of the mechanisms are separated and performed by different parts. There are also limitations and drawbacks however to these types of mechanisms. Separate parts have to be assembled and this introduces additional costs. Size restrictions also have to be considered, as more complex manufacturing and assembly procedures are necessary when parts are

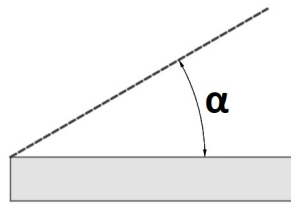


Figure 1.1: Overhang angle defined as α .

miniaturized. Moving parts may have to be lubricated to reduce friction and lubricants can degrade over time and contaminate other parts, the quality and coating of optical surfaces can be diminished by out-gassing of lubricants for example. The stacking of parts can also reduce the overall stiffness of a mechanism and increase tolerances, which leads to less precise mechanisms. Using multiple parts can also introduce mismatched thermal properties such as unwanted temperature sensitivities or cause stick slip effects due to different thermal time coefficients during thermal cycling.

Compliant mechanisms are often used as an alternative to conventional mechanisms in precision and/or miniaturized applications. Compliant mechanisms use flexures as their hinges instead of rigid bodies. Movement is achieved through the elastic deformation of these flexures. This results in compliant mechanisms being precise and predictable [9], [11], and makes them suitable for the alignment that is needed in high performance optical systems. Because movement is achieved through elastic deformation, there is no intrinsic need for multiple parts. A compliant mechanism can be manufactured as one monolithic part. This eliminates friction and the need for lubrication, making them suitable for low-pressure environments or where little to no maintenance is a requirement such as in space applications. It also reduces the costs associated with the assembly of mechanisms.

The design and use of compliant mechanisms comes with its own challenges. Because they are different from conventional mechanisms, some designers may find creating a compliant mechanism to be unintuitive. It can be more difficult to determine the resulting motion of a compliant mechanism than a rigid-body design. When large deflections happen in flexures they can no longer be approximated with linear equations. This can cause additional design tools such as FEM analysis to be used in earlier design stages than they otherwise would be. Motion and force are intertwined in a compliant mechanism and the storage of elastic energy in a deflected position can be problematic. One example of this is the unwanted deformation of a compliant mechanism due to stress relaxation in its flexures. Fatigue also needs to be considered in compliant mechanisms that will go through multiple deformation cycles. The reduced part count of compliant mechanisms can result in multiple functions and movements to be performed by one part or flexure. This complicates the design process as more requirements have to be considered to reach an optimum. The range of motion is also considerably more limited than those of conventional mechanisms.

1.3. Influence of manufacturing technologies

The features and characteristics a part can have are determined largely by its manufacturing method. Different manufacturing methods introduce different sets of freedoms and constraints on a design. This chapter will discuss three methods by which compliant alignment mechanisms are produced; machining, spark erosion and metal 3D printing. Benefits and shortcomings of all techniques are discussed with the emphasis being on the capabilities and challenges of metal 3D printing.

1.3.1. Machining

Machining is the oldest and most widely used manufacturing method among those discussed in this chapter. Because of this, most design challenges that could be solved with machining, have been solved with machining. This has resulted in large body of work to reference. Designers are generally familiar with the constraints and freedoms of the machining process. Machining can be done on a wide selection of metals, plastics, ceramics and composite materials. It is a subtractive process, where material is removed from a piece of stock with a tool. For some designs this can result in large amounts of waste material, which adds both material and machine time costs. Costs are also strongly correlated to geometric complexity, requiring more advanced machines and more machine time to produce geometrically complex features on a part. Cutting tools require access and clearance to create a feature in a part, splitting a part into multiple components to allow the cutting

tool access to the features to be machined is in some cases the only way to create certain geometries. Splitting a part into multiple pieces makes it non-monolithic, the drawbacks of which are mentioned in section 1.2.

1.3.2. Spark erosion

Spark erosion, also known as Electrical Discharge Machining (EDM), is another subtractive manufacturing process. A rapid series of electric arcs is generated between the tool and the part which are separated by a dielectric liquid. This electric arc can remove material in a very controlled manner. Due to the working principle, EDM is only compatible with electrically conductive materials. There are two types of EDM: Wire and Die sink. The main difference between them is the type of tool that is used. Wire EDM uses a thin wire between two guides that is constantly fed from a spool to prevent tool erosion and is held in a straight line by tension. The position of the guides can be controlled on some machines to change the angle of the wire during machining. Die sink EDM uses a larger electrode as its tool. This electrode is lowered onto the workpiece as erosion due to the electrical discharges progresses. A benefit of spark erosion is that it can produce parts with high tolerances on their dimensions and surface quality. Wire EDM is suited for the production of mechanisms that can be described by a single 2D drawing where material only needs to be removed in the direction of a single axis. If a design requires material to be removed in the direction of a second axis, the final part sometimes needs to increase in size as the machine paths on the two different planes cannot intersect each other. Die sink EDM has a similar limitation on geometries it can produce as machining; the tool requires both clearance and access to machined features.

1.3.3. Metal 3D printing

Process overview

There are two main types of metal 3D printing processes: Direct Energy Deposition (DED) and powder bed fusion (PBF).

DED processes create geometries by melting material as it is being deposited [6]. In the process one or multiple nozzles are used to feed powder to the substrate. A focused heat source, typically a laser or electron beam, creates a melt pool on the surface of the substrate. The powder flow is directly deposited into this melt pool. The general DED process is illustrated in figure 1.2. Because material is deposited onto the substrate with a traveling melt pool, the parts created with the DED process have a high density. Because the kinetic energy of the powder flow outweighs the effects of gravity on the particles the material can be deposited in any angle.

The Powder Bed Fusion processes manufacture parts by depositing a layer of powder onto a substrate which is then selectively molten by a heat source. This is the main difference compared to DED, where the feedstock is added to a melt pool. The main PBF process is selective laser melting (SLM). The SLM process is schematically illustrated in figure 1.3.

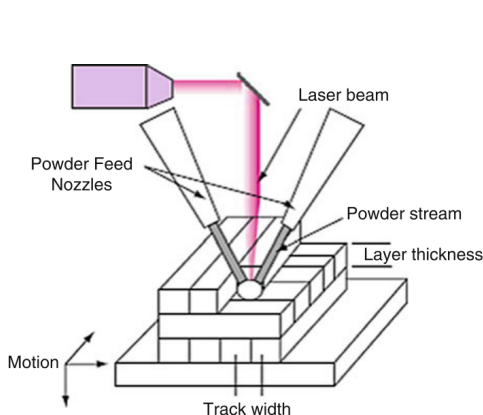


Figure 1.2: Schematic of a typical laser powder DED process [6].

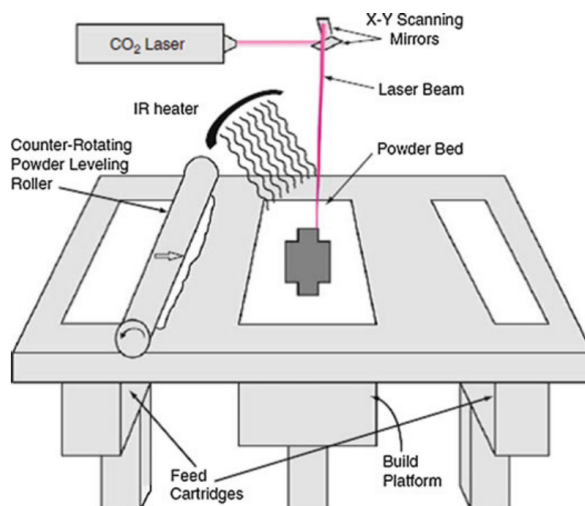


Figure 1.3: Schematic of the selective laser sintering process [6].

The SLM process uses a laser as its heat source. The powder feedstock is spread across the build area with a counter-rotating roller. The laser traces a cross section of the part upon a deposited layer of powder feedstock

which melts the particles together and to the previous layer. This process happens inside an enclosed build chamber which is filled with an inert gas such as nitrogen to minimize oxidation. To minimize warping the powder is kept at a temperature slightly below its melting point by infrared heaters. The build platform can also be heated. Elevating the temperature also minimizes the energy the laser source needs to provide to melt the powder feedstock together. After a layer is completed the build platform lowers by the height of one layer and another layer of powder feedstock is deposited with the roller. This process is repeated until the part is complete. The microstructure achieved with the SLM process is similar to DED processes [6].

SLM and its derivatives are the most widely used processes for the manufacturing of metal 3D printed parts. Because of this the rest of this report will focus on SLM.

Limitations

The metal 3D printing process can produce monolithic parts with great geometrical freedom but is limited in what it can achieve in some aspects. The layer by layer nature of the manufacturing process, the powder feed stock and the use of high power lasers all introduce unique design constraints.

Overhang

The main limitation with metal 3D printing processes is the limited capability to produce overhanging geometries. The critical overhang angle, below which defects occur, is between 60° and 30° depending on the used machine and material, with Titanium alloys generally allowing for the lowest overhang angles [1]. When geometries do not have sufficient support, either from material in the previous layer, powder or support structures, fabricating defects occur. The three main defects that happen when overhanging geometries are made are dross formation, the staircase effect and warping. Dross formation happens when the laser irradiates areas that are supported by powder. Powder supported areas have much lower heat conduction than those that are supported by solid material. This results in more absorbed energy in powder supported zones, which leads to larger melt pools which sink into the powder layer due to capillary forces and gravity [4]. This process is illustrated in figure 1.4. The formation of dross results in lower dimensional accuracy and higher surface roughness in areas that have overhanging surfaces.

The staircase effect is a result of the layer by layer process of SLM metal 3D printing. When the CAD model is sliced into layers its sloped surfaces are approximated with steps. This effect becomes more pronounced when the slope becomes more shallow or when the layer thickness is increased. This effect is illustrated in figure 1.5. The difference between the CAD model and the manufactured surfaces is due to the height of the cusps, as shown in figure 1.5. On thin features, leaf flexures for example, the difference in geometry between the printed and CAD model can be relatively large. How the slicer software interpolates sloped surfaces with layers and how the cusps are positioned is therefore an important design consideration in 3D metal printing.

The warping effect happens due to thermal stresses that accumulate as subsequent layers are deposited. The top and bottom of a new layer are exposed to different rates of heat conduction which results in the top part warping the lower part of the layer. When there is an overhang present in the part this warping accumulates and can lead to a significant change in geometry. This is one of the mechanisms that limits the overhang angle with selective laser melting manufacturing methods. The warping can be mitigated by lowering the energy input but only up to a certain point, as too low energy input results in a weak bond between layers. [13]

There are three main strategies to prevent and minimize dross formation, warping and the staircase effect. The first option is re-orienting the part on the build plate. The geometry in figure 1.4 for example can be rotated 45 degrees counterclockwise to avoid overhanging geometries. Re-orienting can either aim to evenly distribute the overhang over the whole part to avoid re-design and support material entirely, or concentrate all the overhang on one area of the part such that only a partial re-design or a small amount of support material

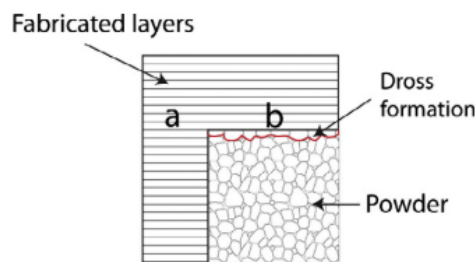


Figure 1.4: Dross formation on an overhanging surface [4].

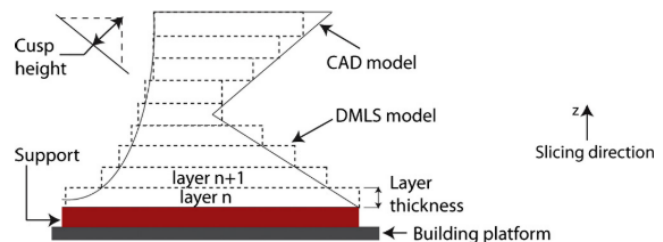


Figure 1.5: Staircase effect when a CAD model is sliced [4].

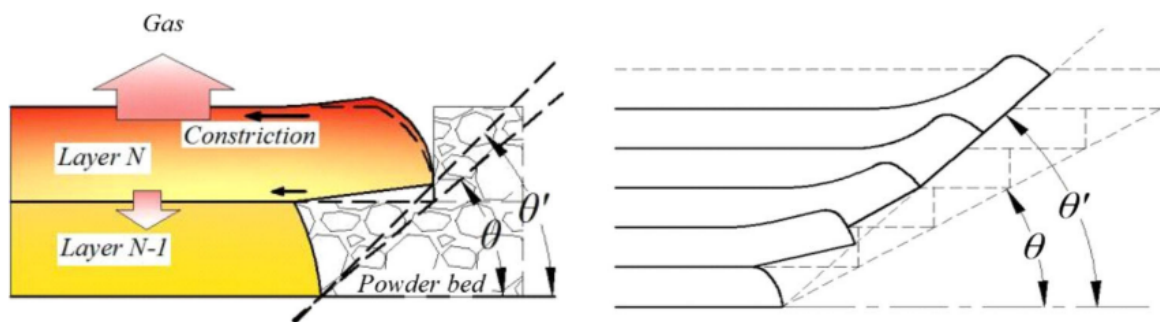


Figure 1.6: (a) Warping of overhang in one layer (b) Accumulation of warping in multiple layers [13].

is needed. A (partial) re-design should be considered if steep overhangs cannot be avoided throughout the design by re-orienting alone. If a re-design is not feasible, support material can be used to ensure overhanging features print without major defects. Support material must be easily detachable from the part while being stable at the same time. Many slicing programs provide the option to auto-generate support structures on overhanging areas that exceed a set angle. In some cases the auto-generated support may not be sufficient and placing custom support within the slicer software or designing support structures manually into the part may be necessary.

Not all overhangs result in prohibitive manufacturing defects. In a paper by M. Dana, I. Zetkova and P. Hanzl [5] it was found that rectangular overhanging ends of less than 0.6 mm printed without significant deviations from their intended geometry and overhangs of up to 1 mm also succeeded, although with increasingly worse surface quality. Overhangs larger than 1 mm failed to print successfully. These results for 90 degree overhangs imply that it would also be possible that notch hinges with radii of up to 2 mm, with the part overhanging beyond 30 degrees being half the radius, can be printed without the need for support structures. This result is corroborated by D.Thomas [12] in his Ph.D. thesis "The development of design rules for selective laser melting", where it is stated that concave radii up to 3mm can be printed with some success. For better results an alternative geometry, depicted in figure 1.7, with different parameters for various overhang distances is proposed. When the radius of a fillet for an overhanging ledge exceeds 5mm, a 45° chamfer should be used instead.

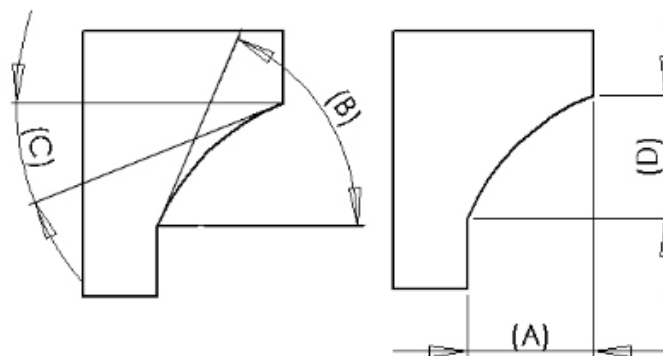


Figure 1.7: An alternative geometry to concave fillets [12].

Feature size

During the SLM printing process, powder feedstock is molten into droplets which form the features of a part. The minimum feature size is limited by the size of these droplets and the interaction between them as the features must be much larger than the droplets, which in their turn must be much larger than the powder particle size.

The minimum achievable size for positive features, such as walls and rods, is between 0.2 and 0.4 mm. Whether a feature prints correctly depends on multiple factors: a short wall with 0.2mm thickness that is supported on both sides might print correctly, but a free standing pillar of the same thickness and even up to 0.5mm can fail [1], a thin wall printed at a 45°angle is also more prone to failure than one printed upright. A

good rule of thumb in this case would be to take 0.5mm as the minimum feature size [12].

There is also a minimum gap size needed between features to ensure that they do not merge together. This minimum size is 0.3 mm [12] in most cases. For circular holes this minimum size changes. Flat lying holes have a minimum size between 0.3 and 0.7 mm, depending on the specific machine, before they fuse shut. Upright holes have a minimum size of 1mm before they are no longer recognizable.

Holes are not self supporting in the upright orientation. Limiting the size of upright holes ensures that the defects due to overhang have too few layers to accumulate in a significant way. The largest possible hole that can be printed without support is between 7 and 8 mm diameter [12][1].

There is another limit on feature size. Large cross sectional areas in a part can cause deformations due to thermal stresses. This problem can be solved in three ways: Adding a rigid support structure to limit deformations until the thermal stresses can be relieved with a heat treatment, re-orienting the part in such a way that the largest cross sections are no longer in the horizontal plane or altering the part by removing material.

Influence on design

Metal 3D printing as a manufacturing technique introduces unique design freedoms and constraints. The design space is sizeable due to the lack of a conventional tool that needs clearance and access to form features on a work-piece. Machine time and costs are strongly correlated with the height of a part and less with its geometric complexity. This means that parts can be very geometrically complex at little additional cost. Additionally, parts produced by metal 3D printing are monolithic and possess all the positive qualities associated with that as described in section 1.2. Lead times for metal 3D printed parts also tend to be shorter than those for machining or spark eroding. Difficulties with designing parts for metal 3D printing partly originate from one of its benefits; the large design space. This design space is non-conventional and dictated by the build direction. Because there are so many geometries possible it can be difficult to map all the relevant solutions to a problem and choose the best one. When the strengths and weaknesses of metal 3D printing are considered, problems often can not or should not be solved in the same way as they would with conventional manufacturing techniques.

1.4. Research goal

The large solution space for metal 3d printed alignment mechanisms can pose difficulties during design. Design methods such as FACT [7] solve similar problems in flexure design. This study aims at developing a complementary design method, specifically for 3D printing, to help designers use the large solution space of metal 3D printing to create compliant alignment mechanisms. The overarching goal is to develop a design method with building blocks, guidelines and strategies to solve problems related to compliant alignment mechanisms for metal 3D printing. This paper is intended to make a start towards achieving this goal. This start should consist of a basic set of printable building blocks, a system to order these elements and a method to use them to develop concepts for compliant 3D printed alignment mechanisms.

1.5. Approach and structure

The main body of this thesis consists of a research paper. This paper contains a shorter introduction that touches on the main points that have already been discussed in this first chapter. The contents of chapter two through four are exclusively contained in the research paper. An expanded version of the conclusion and recommendations section of the paper is added at the end of this thesis report.

The structure of the research paper is as follows:

In chapter two a method of structuring building blocks is presented followed by the tools needed to construct building blocks and the building blocks themselves. These are then presented in three complementary tables. The chapter is concluded by a design method for applying the tables and building blocks towards the development of concepts for metal 3D printed compliant alignment mechanisms. Chapter three demonstrates the design method by applying it to an example case. The example is developed by stating design requirements, developing concepts using the design method and integrating them into a conceptual design that complies with the design requirements. This conceptual design serves as a starting point for optimization or creative design alterations. Chapter four explores some of the properties of the conceptual mechanism developed in chapter three using finite element analysis and a prototype manufactured in Ti6Al4V. In the final chapter the results of the previous sections are interpreted followed by a set of recommendations for future research.

1.6. Definitions

Some words that are used extensively in the paper are defined in this section.

Constraint combination: A constraint combination specifies which of the six degrees of freedom are constrained for a moving body.

Strut configuration: A strut configuration visually represents the constraints on a moving body with strut flexures. Each strut configuration is paired with a constraint combination.

Substitution element: Substitution elements are flexures that apply equivalent constraints on a moving body as a specific strut configuration.

Printable building block: Printable building blocks are defined as one or more flexures connected to a moving body and the fixed world, and constrain a specific combination of DoF. Such building blocks enable the designer to combine them to create concepts for compliant mechanisms. Only the flexures are subjected to the self-supporting angle requirement of at least 45 degrees.

Overhang angle: The overhang angle refers to the angle between the horizontal plane and the downfacing surface of a printed geometry. It is defined as angle α in figure 1.1.

Start of paper

This thesis is partially written in the format of a paper and is intended to be published in the precision engineering journal. Because the paper is written in a different format and has to be self-contained, the bibliography is split between the thesis and paper. The numbering for chapters and figures also resets with the start of the paper to maintain accurate cross-references within the paper.

The printable building blocks presented in the paper have been developed over the course of this thesis project. FDM 3D printed models have been very helpful during this process to inform and guide design decisions. As these FDM 3D prints are not included in the contents of the paper they are instead presented here in figure 1.8.

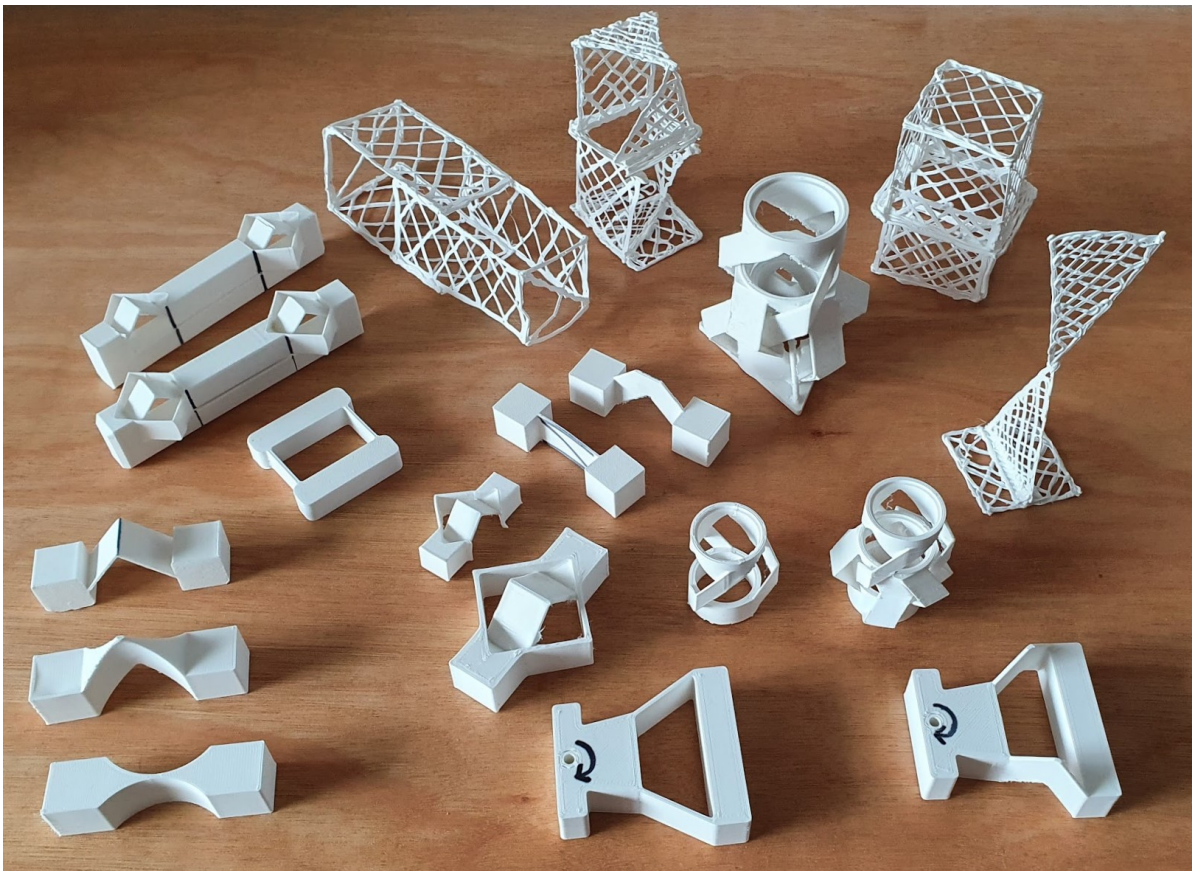


Figure 1.8: A selection of FDM 3D prints used to develop building blocks over the course of this thesis.

Design method for 3D printed compliant mechanisms^{*}

T.R. Oude Vrielink^{*} (Student), dr. ir. L.A. Cacace^{**} (Supervisor)

ARTICLE INFO

Keywords:
metal 3D printing
SLM
compliant
alignment
optics
flexure

ABSTRACT

There are strict tolerances on the placement of optical components in high performance optical systems. Compliant alignment mechanisms can be used to meet these tolerances. Conventional manufacturing techniques, such as milling and spark erosion, have been used to produce an extensive library of alignment solutions but are limited in the geometries they can produce. Metal 3D printing (SLM) is a newer manufacturing method that can produce complex geometries in a large design space with unique limitations but has no extensive library of solutions. A design method is proposed to construct building blocks for concept generation as a foundation for this library. The method aims at achieving this by reducing the size of the solution space, dividing it into separate constraint combinations. These constraint combinations and tools to develop them into building blocks are presented as tables with geometries and a flowchart describing their use. The design method is demonstrated by applying it towards the development of a compact, low-mass mechanism with three independent alignment stages. FEM analysis and a prototype in Ti6Al4V are used to explore some of the properties and manufacturability of this demonstration case.

1. Introduction

1.1. 3D printing for OM

Optical components are used in many different applications such as satellite imaging, scientific instruments, industrial manufacturing and medical applications. Because the wavelength of light is in the sub-micrometer range, some of the tolerances on high performance optical systems are in the micro- to nanometer range. To reach the desired performance in these systems, the optical components have to be placed within these tolerances and alignment is one of the methods of achieving this. Multi-body mechanisms consisting of conventional hinges and couplings have many applications in which they are very useful but have some distinct disadvantages when applied in high precision systems. The assembling of multiple parts can introduce lower overall stiffness in the mechanism, friction in moving parts, mismatched thermal properties, thermal barriers, stacking of tolerances and extra costs. Compliant mechanisms provide a solution to these issues [10], [12]. Compliant mechanisms function through the elastic deformation of flexures which are compliant in some directions and stiff in others. Everything but the desired direction of movement can be constrained by arranging these flexures in a specific manner. Because movement is achieved through elastic deformation, compliant mechanisms can be made as monolithic parts. This enables them to be predictable and operate without friction or play. Compliant mechanisms are usually made with conventional manufacturing techniques such as milling and spark erosion. These methods have limitations which makes some geometries considerably expensive or impossible to manufacture. Splitting a monolithic design into multiple parts can be the only way to manufacture it with conventional techniques in some situ-

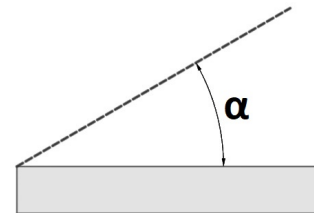


Figure 1: Overhang angle defined as α .

ations. Metal 3D printing is a newer manufacturing method with unique capabilities and limitations. The process considered in this paper is selective laser melting (SLM). It can produce monolithic parts with great geometrical freedom but is limited in what it can achieve in some aspects. The layer by layer process, the powder feed stock and the use of high power lasers all introduce design constraints [5]. The main limitation with metal 3D printing processes is the limited capability to manufacture overhanging geometries. The critical overhang angle is between 60° and 30° , defined as angle α in figure 1, depending on the particular machine and material. When geometries are below this self-supporting angle, fabricating defects occur. Titanium alloys generally allow for lower overhang angles [2], are suitable for creating flexures due to their ratio between yield strength and youngs modulus [8], [4], and are compatible in thermal expansion coefficient with many glass types [3], [11]. The compliant mechanisms that can be produced with conventional methods are well documented and known. This is not yet the case for metal 3D printing. The solution space is defined by new rules, is quite large and not fully explored. These factors present obstacles for designers in making effective use of metal 3D printing for the production of alignment mechanisms.

^{*}This research project is funded by TNO

^{*}Corresponding author

^{**}Principal corresponding author

 thijsoudevrielink@gmail.com (T.R.O. Vrielink);

l.a.cacace@ac-optomechanix.com (L.A. Cacace)

ORCID(s):

1.2. Research goal

The large solution space for metal 3d printed alignment mechanisms can pose difficulties during design. Design methods such as FACT [6] solve similar problems in flexure design. This study aims at developing a complementary design method, specifically for 3D printing, to help designers use the large solution space of metal 3D printing to create compliant alignment mechanisms. The overarching goal is to develop a design method with building blocks, guidelines and strategies to solve problems related to compliant alignment mechanisms for metal 3D printing. This paper is intended to make a start towards achieving this goal. This start should consist of a basic set of printable building blocks, a system to order these elements and a method to use them to develop concepts for compliant 3D printed alignment mechanisms.

1.3. Approach and structure

In section two a method of structuring building blocks is presented followed by the tools needed to construct building blocks and the building blocks themselves. These are then presented in three complementary tables. The section is concluded by a design method for applying the tables and building blocks towards the development of concepts for metal 3D printed compliant alignment mechanisms. Section three demonstrates the design method by applying it to an example case. The example is developed by stating design requirements, developing concepts using the design method and integrating them into a conceptual design that complies with the design requirements. This conceptual design serves as a starting point for optimization or creative design alterations. Section four explores some of the properties of the conceptual mechanism developed in chapter three using finite element analysis and a prototype manufactured in Ti6Al4V. In the final section the results of the previous sections are interpreted followed by a set of recommendations for future research.

1.4. Definitions

Some words that are used extensively in this paper are defined in this section.

Constraint combination: A constraint combination specifies which of the six degrees of freedom are constrained for a moving body.

Strut configuration: A strut configuration visually represents the constraints on a moving body with strut flexures. Each strut configuration is paired with a constraint combination.

Substitution element: Substitution elements are flexures that apply equivalent constraints on a moving body as a specific strut configuration.

Printable building block: Printable building blocks are defined as one or more flexures connected to a moving body and the fixed world, and constrain a specific combination of DoF. Such building blocks enable the designer to combine them to create concepts for compliant mechanisms. Only the flexures are subjected to the self-supporting angle requirement of at least 45 degrees.

Overhang angle: The overhang angle refers to the angle between the horizontal plane and the downfacing surface of a printed geometry. It is defined as angle α in figure 1.

2. Building blocks

Compliant mechanisms are usually designed by combining individual flexures and simple flexure mechanisms. These individual flexures and simple flexure mechanisms can be viewed as the building blocks of a conceptual design. Because metal 3D printing imparts new constraints and new freedoms on the design space, a set of printable building blocks functionally equivalent to the conventional flexures and mechanisms would aid in the effective use of this new design space. This chapter will discuss this set of printable building blocks and its prerequisites and present them in complementary tables. These tables are included at the end of chapter 2 due to their size. These printable building blocks are conceptual in nature and follow the assumption that overhang angles of 45 degrees are acceptable. If the material and/or process allows for lower overhang angles, the printable building blocks can be optimized for this as needed in later design stages.

2.1. Structuring approach

The goal is to construct a set of printable building blocks that can be used to create concepts for compliant alignment mechanisms. Alignment mechanisms can be categorized by their combination of free and constrained DoF. Just as one type of alignment can be done by multiple types of alignment mechanisms, each of these constraint combinations can result in multiple printable building blocks. All of these constraint combinations must be considered to prevent printable building blocks from being missed. The first step in creating the desired set of printable building blocks is therefore to divide the complete freedom and constraint space in constraint combinations using 6 independent DoF. Each of these constraint combinations is represented conceptually by a coordinate system showing the constrained DoFs, referred to as a constraint representation, and physically by a configuration of strut flexures. These strut configurations are constructed from one or more strut flexures in parallel that constrain a central moving body. Struts are used because they are the simplest physical shapes that constrain one DoF. The constraint combinations and strut configurations are presented in a table that is sorted by number of unconstrained DoF in section 2.2.

The next step is converting the strut configurations to printable building blocks. This is done through the use of substitution elements. These elements are equivalent to and replace specific configurations of struts. For this process to result in printable building blocks, the substitution elements themselves have to comply with the design constraints of the metal 3D printing manufacturing process. An overview of some of the geometries that fulfill these requirements is presented in section 2.3.

The printable building blocks can be created with the constraint combinations represented by strut configurations

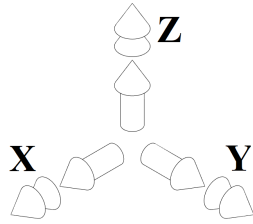


Figure 2: Definition of coordinate system.

and the substitution elements. Because there are multiple constraint combinations, each of which can result in multiple printable building blocks for each considered orientation, the complete library would consist of dozens of printable building blocks. To manage the scope of this paper, the number of constraint combinations to be converted has been restricted to five cases. These five correspond to the same DoF as the five most basic flexures, namely:

- Strut
- A-type/notched leaf
- Leaf
- Pin
- Notch

These five flexures are used to construct most compliant mechanisms and are used as a foundation for the complete set of building blocks.

Each constraint combination that corresponds to one of the five basic flexures is converted to a set of printable building blocks for three orientations. The results are presented in a table with the conventional flexures and their corresponding printable building blocks. The tables with constraint representations and printable building blocks, in section 2.2 and 2.4 respectively, omit serial solutions to prevent the same information from being included twice. For example, the set of solutions for tip/tilt mechanisms would not include two notch flexures combined in series. The naming convention for constraints is $T_x T_y T_z$ for translations and $R_x R_y R_z$ for rotations. The x-, y- and z-axis are defined as in figure 2.

2.2. Constraint representation by strut configurations

As mentioned in section 2.1, the first step in structuring the design space for metal 3D printed compliant mechanisms is dividing the complete freedom and constraint space into separate constraint combinations. To prevent duplicate entries, constraint combinations resulting from rotational or reflectional symmetry are disregarded. This results in 18 unique combinations of 6 independent DoF. These constraint combinations are represented by strut configurations in which combinations of parallel struts are used to constrain a moving body. Some constraint combinations cannot be constructed without using intermediate bodies. Only for these constraint combinations the structure in figure 3, which constrains a

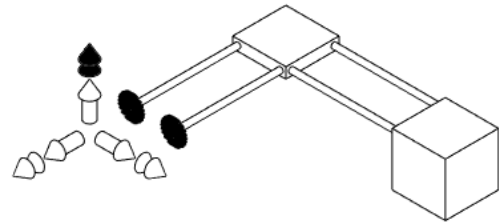


Figure 3: One rotation constrained by two sets of two struts in series.

single rotation without constraining a translation, is used in addition to single struts to create a strut configuration. Table 1 contains all constraint combinations and strut configurations and is included at the end of chapter 2.

2.3. Substitution elements

Converting the constraint representations to printable building blocks requires the replacement of struts by other geometries. These geometries are the substitution elements. Most flexures and compliant mechanisms can be constructed by combining these elements. For the building blocks to be printable, the substitution elements themselves must comply with constraints on the metal 3D printing process. The dominant constraint on printable geometries is the overhang angle. An overhang angle of 45 degrees is assumed to be acceptable and concepts resulting from the building blocks can later be adjusted for lower overhang angles if desired. The first members of the substitution elements are simple geometrical shapes analogous to the five basic flexures as defined in section 2.1. In the same order as those five flexures, they are:

1. Strut
2. Triangular plate
3. Rectangular plate
4. Cone
5. Triangular prism

These five substitution elements are illustrated in table 2. Some of these elements have orientations in which they are not printable. The strut, rectangular plate and triangular prism all require modifications to comply with the 45 degree overhang angle constraint in some orientations. To solve this, the rectangular plate and triangular prism can be skewed by 45 degrees to become self supporting, resulting in substitution elements 6 and 7 respectively in table 2. The strut cannot be printed in the horizontal position. There are two options for alternative geometries that apply the same constraint as a strut. The first option is a folded rectangular plate, element number 8 in table 2. Because the two plates are connected in series at a 90 degree angle, the only DoF that is constrained by both plates is the translation along the fold line. This element can be oriented such that both plates have a 45 degree overhang and are self-supporting.

The second option is an hourglass flexure (substitution element number 9 in table 2) and it is similar to the folded rectangular plate. Two planes are joined at an angle and

share one common constrained DoF. The element can be viewed as a strut flexure with built-in support that does not need to be removed. To improve robustness, the joint between the two plates can be made thicker without adding additional constraints. This type of flexure can also be a replacement for vertical or angled struts (substitution element number 10 in table 2). A possible benefit of an hourglass flexure is that it provides a larger surface for subsequent non-compliant bodies to be built from compared to a strut. A possible drawback is that an hourglass flexure is less compliant than a strut of the same thickness and overall length. The lower compliance is due to each of the halves of the hourglass flexure being half of the overall length. This lower compliance can be compensated for by printing the hourglass flexure at a lower wall thickness. This is possible because walls are more robust than cylinders, which results in the minimum wall thickness being lower than the minimum diameter of cylinders [2], [13]. The hourglass can be an alternative to struts in any orientation if the extra volume claim compared to struts does not interfere with other bodies.

Another alternative to a strut in the vertical direction would be a folded rectangular plate. This element is not printable in this orientation however due to a 0 degree overhang. This can be solved in the same way as the rectangular plate and triangular prism; by skewing it. This results in a skewed folded rectangular plate, substitution element number 11 in table 2. This element can be an alternative to a vertical strut if the space directly between the attachment points of the flexure on the guided body and fixed world is not available. Because the compliant members are angled, parasitic motion in the z-axis is lower for a given horizontal deflection than a that of a strut of the same height.

The substitution elements are listed in table 2 in order of introduction. This table is included at the end of chapter 2.

2.4. Printable building blocks

The printable building blocks are made by replacing the struts from the strut configurations with the printable substitution elements until there are no more flexure elements left that do not comply with the overhang constraint of 45 degrees. There are 18 constraint combinations represented by strut configurations and each can be converted into multiple printable building blocks depending on the choice of substitution elements and the considered orientation. Converting all strut configurations in every orientation would result in dozens of printable building blocks. The scope of the printable building blocks overview has been limited by only considering printable equivalents to a set of five conventional flexures. These flexures are:

- Notch
- Leaf
- Pin
- A-type/notched leaf
- Strut

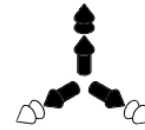


Figure 4: Tx, Ty, Tz and Rz constraints for tip tilt alignment.

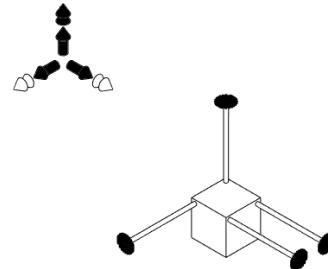


Figure 5: Constraint representation and strut configuration number 5, tip tilt in x- and y-axis.

These flexures are already printable in some orientations but require conversion to printable equivalents for others. The printable orientations for the conventional flexures together with the printable equivalents for other orientations create a set of printable building blocks from which most compliant mechanisms can be constructed for the metal 3D printing process. They are presented in table 3 with the conventional flexures and the three considered constraint orientations. If printable building blocks have reflectional symmetries, only one is included in table 3 to prevent duplicate information. The table is included at the end of chapter 2.

2.5. Design method

The general method to generate building blocks for metal 3D printed compliant alignment mechanisms is described with a flowchart in figure 10 at the end of chapter 2.

The design method is demonstrated by developing printable building blocks for the concept selection of a tip tilt alignment mechanism that aligns tip in the x-axis and tilt in the y-axis.

Step 1B: Determine the desired constraints. For this tip tilt alignment the constraints are Tx, Ty, Tz and Rz, illustrated in figure 4.

Step 2B: Choose between a parallel or serial combination of flexures. Both cases will be considered in this example. A parallel flexure combination is chosen first.

Step 3B: Determine if the constraints listed in step 1B are equivalent to one of the conventional flexures in table 3: notch, leaf, pin, A-type or strut. This is not the case.

Step 4B: Select corresponding strut configuration from table 1, in the case of a tip tilt alignment this is number 5. The constraints as depicted in this strut configuration are already aligned with the desired constraints so rotation is not needed.

Step 5B: Rotate 45 degrees about x- or y-axis for alternative strut configurations. Rotating around one of these axes changes the direction of the constraints. If the constraint rep-

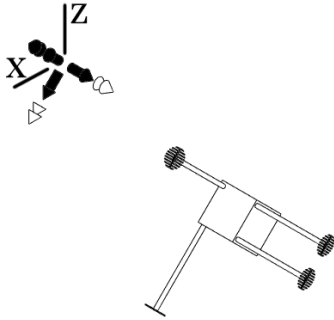


Figure 6: Alternative strut configuration for tip tilt alignment created by rotating 45 degrees around the y-axis.

resentation and strut configuration are rotated around the y-axis, as seen in figure 6, the tilt alignment remains the same. The tip alignment is now in the xz-plane and results in a rotation around both the x- and z-axis, which projects part of the tip alignment in the x-axis onto the tilt alignment in the y-axis. Because the tilt alignment is still independent, this parasitic rotation imparted on the y-axis through tip alignment can be compensated. Thus, tip tilt alignment can still be achieved at the cost of an extra iteration step during the alignment process.

Step 6B: For each strut configuration, replace all struts with substitution elements until all flexures comply with self-support rules. The strut configurations to be converted are those in figure 5 and 6. Each strut configuration can be converted to multiple printable building blocks. Converting the strut configurations in figure 5 and 6 results in the printable building blocks depicted in figure 7.

For a complete overview of the solution space, step 2B is considered again.

Step 2B: Choose between a parallel or serial combination of flexures. Both cases will be considered in this example. A serial flexure combination is chosen.

Step 3C: Split the constraints from step 1B into multiple constraint combinations in series. The constraints can be split into two cases: Rx unconstrained in series with Ry unconstrained.

Step 4C: Follow the flowchart for each case.

Case 1: Ry unconstrained

Step 1B: The new constraints are Tx, Ty, Tz, Rx and Rz, illustrated in figure 8

Step 2B: There is only one unconstrained DoF so only parallel flexure combinations are possible.

Step 3B: The constraints are equivalent to those of a notch flexure.

Step 4A: The second row is selected from table 3.

Step 5A: The printable building blocks are added to the solution space

Case 2: Exactly the same as case 1 but mirrored in the vertical plane.

Both cases have now been considered.

Step 5C: Combine the building blocks with intermediate bodies. This results in the printable building blocks depicted in figure 9.

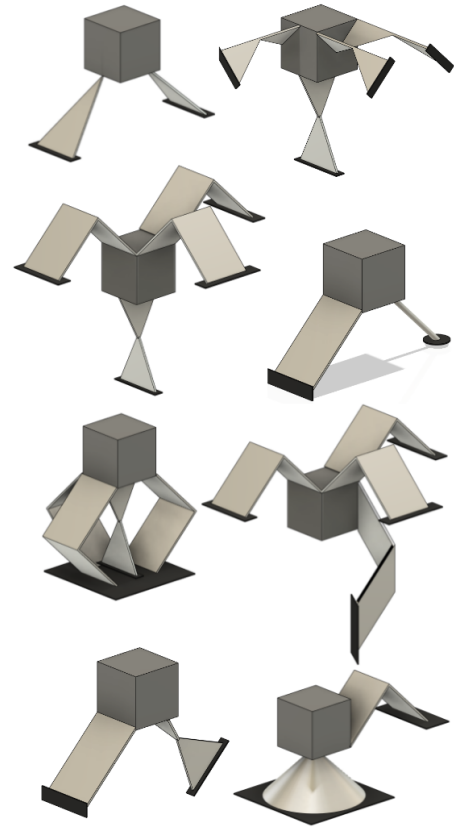


Figure 7: Building blocks with parallel flexure combinations for tip tilt alignment.

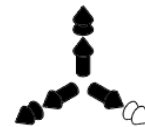


Figure 8: Tx, Ty, Tz, Ry and Rz constrained.

Figure 7 and 9 represent the solution space for an exactly constrained tip tilt alignment mechanism that can be metal 3D printed.

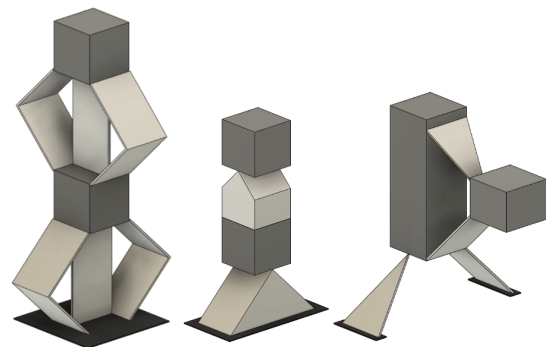


Figure 9: Building blocks with serial flexure combinations for tip tilt alignment.

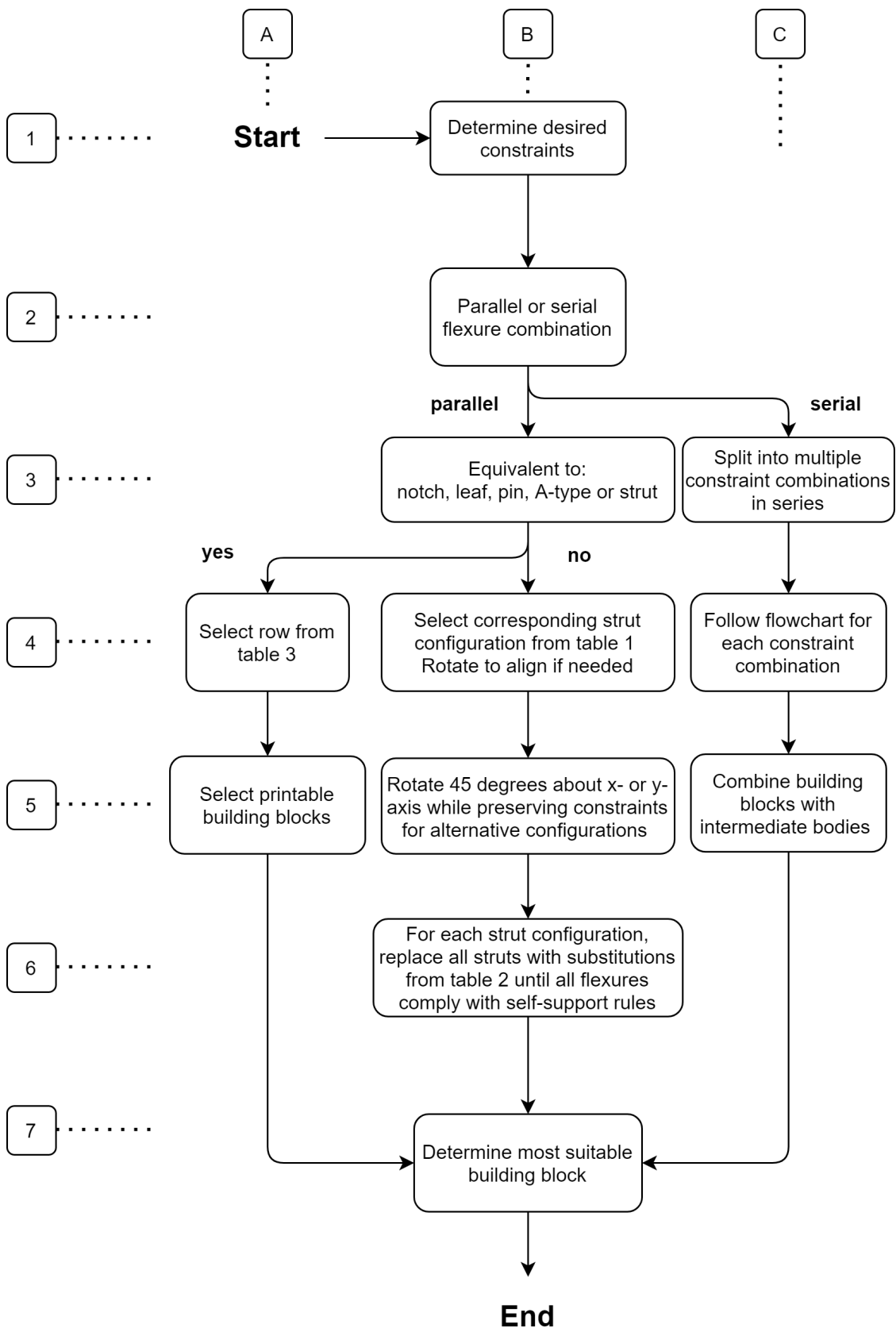


Figure 10: The general design method to generate concepts for metal 3D printed compliant mechanisms.

Free DoF

Constraint combinations and strut configurations

1 DoF	1	2				
2 DoF	3	4	5	6		
3 DoF	7	8	9	10	11	12
4 DoF	13	14	15	16		
5 DoF	17	18				

Table 1
Constraints represented by strut configurations sorted by number of unconstrained DoF.

Constraint combination & Strut configuration	Substitution Element	Constraint combination & Strut configuration	Substitution Element
1 		6 	
2 		7 	
3 		8 	
4 		9 	
5 		10 	
		11 	

Table 2
3D printable substitution elements with corresponding constraint representations and strut configurations, angle $\alpha = 45$ degrees.

Design method for 3D printed compliant mechanisms

	constraint combination	Strut configuration	Conventional hinge	Printable building blocks
Notch				
Leaf				
Pin				
A-type				
Strut				

Table 3
conventional flexures with their DoF equivalent printable building blocks for multiple DoF orientations.

3. Demonstration case

In addition to showing the application of the method described in section 2.5 by developing concepts for a tip tilt mechanism at the end of the same section, the method is also demonstrated by developing an alignment mechanism consisting of multiple alignment stages. The method is used to create printable building blocks which can be used for concept selection for each alignment stage. The concepts are evaluated and a selection is developed and integrated into a conceptual design that complies with the stated design requirements. The chosen types of alignment are: tip tilt, focus and center. These are some of the most basic and often needed alignment types for optical components.

3.1. Design goals

The purpose of the demonstration case is to demonstrate the design method. As such, the details of the optical components are of lesser importance. Simple plano-convex lenses are used with commonly available diameters; 20mm, 25mm and 30mm. The stroke requirement for each stage is similar to other high performance compliant alignment mechanisms for optical elements [9] and is set to $\pm 0.5\text{mm}$ for the focusing stage and centering stage, and $\pm 10\text{mRad}$ for the tip tilt stage. The strengths of the metal 3D printing process are demonstrated by making the mechanism light and compact while also complying with the stroke requirements. The location of thermal centers is often critical in alignment mechanisms. It is preferred if thermal centers of the optical components are located on the optical axis. For this reason the optical axis is set along the z-axis, the same as the build direction. This results in radial symmetry of the overhang angle constraints around the optical axis and allows for more concepts with thermal centers on the optical axis to be considered. A method of actuation is included as a requirement for one of the alignment stages. The last design goal is that the mechanism should be self-contained. This means that the functionality of the mechanism has to remain intact whether it is printed directly on the build plate by itself, or integrated with a larger design. By printing directly on the build plate itself it is possible to split joined parts during the removal from the build plate, allowing for extra design freedom. As this is not a possibility when the design is integrated into a larger component, this extra design freedom will not be considered.

3.2. Tip/tilt concept selection

Following the first step in the design method flowchart shown in figure 10, the desired constraints for tip tilt alignment are T_x , T_y , T_z and R_z , as seen on the left in figure 11. This combination of constraints is referred to as case 1 and is already explored as an example in section 2.5. The R_z constraint in case 1 is not strictly mandatory as the plano-convex lens is not sensitive to rotations around the z-axis. This means that the case where only T_x , T_y and T_z are constrained, illustrated on the right in figure 11, is also considered. This combination of constraints is referred to as case 2.

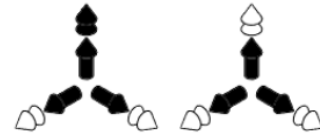


Figure 11: Constraints for tip tilt alignment: case 1 exactly constrained on the left, case 2 with R_z underconstrained on the right.

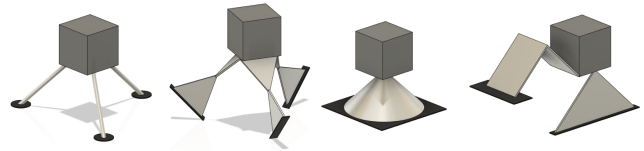


Figure 12: Building blocks with equivalent constraints as a pin flexure.

The second step in the design method calls for a choice between a parallel or serial flexure combinations. For case 2, serial options will combine concepts resulting from case 1, shown in figure 7 and 9, in series with an additional flexure equivalent to a notch. In short, extra complexity is added to create an underconstraint. These serial concepts are less desirable than any solution resulting from case 1 and as such, serial solutions resulting from case 2 will not be considered.

Continuing with the flowchart for case 2, selecting parallel solutions lead to step 3B, which asks if the constraints are equivalent to the constraints of a notch, leaf, pin, A-type or strut flexure, shown in table 3. Because the constraints are equivalent to those of a pin flexure the answer is yes.

The next steps, 4A and 5A, call to select the row from table 3 corresponding to case 2 and select the printable building blocks. There is only one row for pin flexure equivalents. The building blocks in this row, illustrated in figure 12, are thus the concepts resulting from evaluating case 2 with the design method.

Combining the results from from case 2 (figure 12) and case 1 (figure 7 and 9) gives the overview of concepts for a tip tilt alignment stage. Applying the requirement that the thermal center must be located on the optical axis and that the aperture of the lens cannot be obstructed, only the concepts in figure 13 remain. From these, the concept with three angled struts is chosen over the angled three hourglass flexures for its smaller volume claim.

3.3. Focus concept selection

Following the design method for focus alignment, the desired constraints are T_x , T_y , R_x , R_y , R_z , shown in figure 14. There is only one unconstrained DoF, T_z , which means only parallel flexure combinations are possible in step 2B. The constraints for focus alignment are not equivalent to those of a conventional flexure from table 3 in step 3B. Following step 4B, strut representation number 2 is selected from table 1, illustrated in figure 14. The constraints represented by the strut configuration are already aligned to the desired constraints, so no rotation is needed. Step 5B calls for rotating the strut configuration by 45 degrees about the x- or

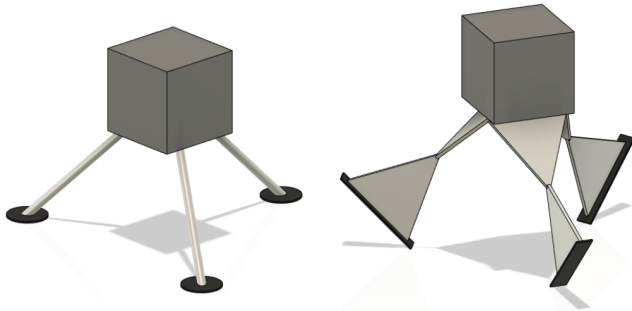


Figure 13: Selection of building blocks used to create a tip tilt stage concept.



Figure 16: Focus stage building block with 6 folded leaf flexures.

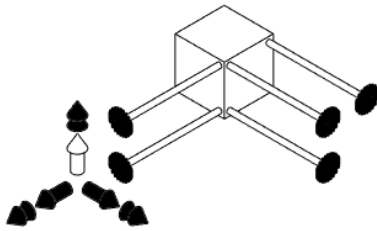


Figure 14: Constraint representation and strut configuration for focus alignment in T_z .

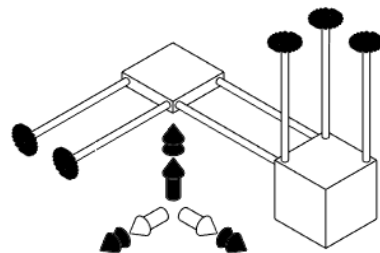


Figure 17: Constraint representation and strut configuration for center alignment in T_x and T_y .

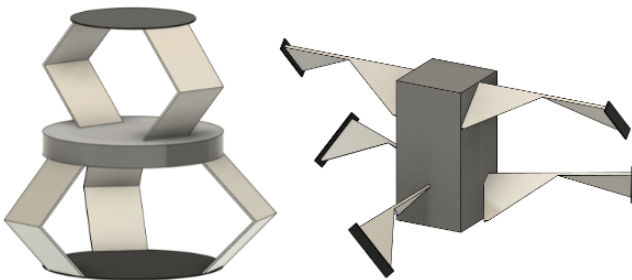


Figure 15: Focus stage building blocks using folded leaf and hourglass flexures.

y-axis and constructing alternative strut configurations. This cannot be done without changing the direction of the focus movement and thus it is not possible to create alternative strut configurations. In the next step, 6B, the struts from figure 14 are replaced by substitution elements until all flexures comply with self-supporting rules. This results in the printable building blocks in figure 15.

The printable building block with folded leaf flexures in figure 15 is chosen because the moving stage can be supported solely by the flexures. An extra folded leaf is added to maintain rotational symmetry of stiffness around the z-axis, resulting in the concept in figure 16. This overconstrains R_z which can be solved by introducing an internal DoF in the moving body. Because the optical element is not sensitive to z-rotation the overconstraint is left as shown in figure 16.

3.4. Center concept selection

Aligning an optical component in center requires constraints on T_z , R_x , R_y and R_z , illustrated in figure 17. Following the design method, step 2B, the parallel options are

explored first. The determined constraints are not equivalent to one of the conventional flexures in table 3. Strut configuration number 6 from table 1, illustrated in figure 17, is chosen in step 4B. The constraints of this strut configuration are already aligned with the desired constraints.

Creating alternative strut configurations in step 5B is not possible as rotating around the x- or y-axis by 45 degrees changes the constraints. The only strut configuration that can be converted to printable building blocks in step 6B is therefore number 6 from table 1 and shown in figure 17. This strut configuration has three vertical struts and four struts in the xy-plane joined by an intermediate body. Converting this to printable building blocks using the substitution elements leads to the building block in figure 18. The three struts in this concept can be kept or replaced by either the hourglass substitution or skewed folded plate elements, number 10 and 11 respectively, from table 2.

Serial flexure combinations that comply with the previously determined constraints are explored next. The constraints are split into two cases, one with T_x unconstrained and one with T_y unconstrained. Following the design method for each case and combining them in series results in the building blocks in figure 19.

Like the tip tilt and focus alignment stages, R_z is not a mandatory constraint due to the insensitivity of the optical element to this DoF. The new set of constraints becomes T_z , R_x and R_y , as shown in figure 20. Because there is an extra underconstraint, all serial combinations for this new set of constraints would be larger and perform worse than those in figure 18 and 19.

Step 4B is next as the new constraints are not equivalent



Figure 18: Exactly constrained centering stage building block.

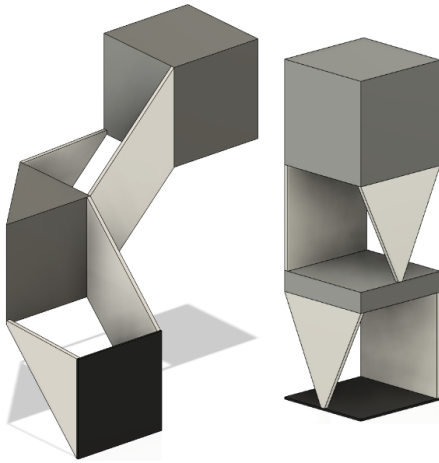


Figure 19: Angled and vertical linear guides in series.

to a conventional flexure from table 3. Strut configuration number 10, shown in figure 20, is selected from table 1. This strut configuration does not need to be aligned in step 4B and cannot be rotated to create alternative configurations in 5B. Converting the strut configuration to printable building blocks is straightforward as there are only vertical struts to substitute. This results in the printable building blocks in figure 21.

From the printable building blocks in figure 18, 19 and 21, the printable building block with three skewed folded leaf flexures shown on the left in figure 21 is chosen. It has a thermal center on the optical axis, is radially symmetric like the chosen concepts for the tip tilt and focus stages, has the lowest amount of parasitic motion in the z-direction, does not have an intermediary body, is most compact in the vertical direction for a given stroke at little cost to compactness in the horizontal plane and the skewed folded plates provide the most freedom for choosing attachment points during the design integration phase.

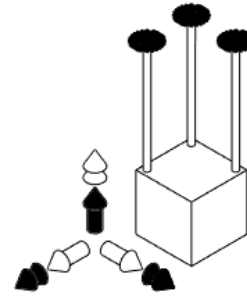


Figure 20: Constraint representation and strut configuration for center alignment in Tx and Ty with Rz underconstrained.

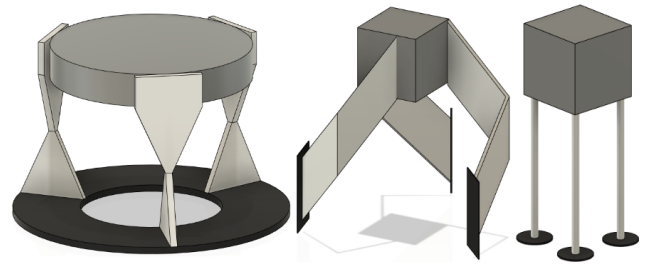


Figure 21: Centering stage under constrained printable building blocks. Left, 3 hourglass flexures, middle 3 skewed folded leaf flexures, right 3 strut flexures.

Measurement	after stress relief	after HIP
Youngs modulus (GPa)	105-120	105-120
Rp0.2% (MPa)		
Horizontal direction	1090 ± 30	910 ± 30
Vertical direction	1080 ± 50	930 ± 30

Table 4
Mechanical properties of Ti6Al4V [1].

3.5. Integrating designs

Integrating the three concepts into one monolithic design requires calculating the dimensions of the flexures and combining the three alignment stages together in one monolithic part. Determining the dimensions of the flexures for each alignment stage starts with material and process properties. The chosen material is Ti6Al4V for its thermal properties, which are a good match with most glasses [3], [11], good ratio of yield strength to youngs modulus [8], [4], and because parts made with Ti6Al4V can be printed with overhang angles as low as 35 degrees [2], which aids a compact, lightweight design. Its mechanical properties are listed in figure 4. The presence of 0.2mm grit on the surface of the metal 3D printed part is assumed [1].

Making the alignment mechanism compact and lightweight is achieved by nesting the three alignment stages inside each other. The diameters for the optical elements are set to 20, 25 and 30mm from bottom to top for this purpose. Each optical element is mounted in a ring that functions as a simple optical mount. These rings are connected to the flexures. For the tip tilt and center stages these rings must be supported from three points. The optical mounts can be made



Figure 22: Mount for circular optical elements which is self-supporting from three initial points.

Stage	Tip Tilt	Focus	Center
Diameter	20 mm	25 mm	30 mm
Stroke	± 10 mRad	± 0.5 mm	± 0.5 mm
Radius	3 mm	n.a.	n.a.
Thickness	n.a.	0.3 mm	0.3 mm
Length	15 mm	8 mm	8 mm

Table 5

Properties of alignment stages and flexure dimensions. Length of folded leaf flexures is defined as in figure 26.

self supporting from three initial points as seen in figure 22. The focus stage can be supported from three lines instead of points which decreases the height of the optical mount.

The order of the alignment stages is determined by investigating how the dimensions of the flexures are dependent on the diameter of the optical mount. The flexures in the tip tilt alignment stage are sensitive to the diameter of the optical mount. As the distance between the virtual center of rotation and the three supporting points of the optical mount increases with diameter, the translation at these supporting points increases as well for the same angular rotation of the moving body. Larger deflections require more compliant flexures to prevent exceeding the elastic deformation range. To achieve the most compact design, the tip tilt alignment stage is paired with the optical mount for the smallest lens. The dimensions of the flexures for the focus and center stage do not depend on the diameter of the optical mount. The order of these stages is therefore chosen arbitrarily with the focus stage in the middle with the 25mm diameter optical element and the center stage on top with the 30mm diameter optical element. The dimensions of the flexures can be determined from the material properties and the manufacturing process. Due to the relatively small deflections of the flexures, linear approximations used in conjunction with a safety factor of 2 are sufficient to calculate the flexure dimensions for the first conceptual design. The resulting dimensions are presented in table 3.5.

Using these dimensions, each stage is modelled sepa-

rately and altered in an iterative manner until the flexures no longer interfere with each other. The three stages are then combined into one monolithic part and a base is added to connect the flexures to the fixed world. An actuation point, as mentioned in the design goals, consisting of a push pull pair is added to the focus stage in the same iterative manner. The resulting mechanism is presented in figure 23.

4. Analysis

The mechanism constructed in section 3.5 shows how the design method can be used to generate concepts and integrate them into a conceptual mechanism. This mechanism is, however, not yet optimized. The dimensions of its flexures were determined through linear approximations and can likely be further improved. This section is used to explore some of the properties of each stage, propose improvements where needed and investigate the effect of these improvements. Because the alignment mechanism is only intended to illustrate the design method, there are no specific requirements on weight, size, parasitic motion, etc. Focus is therefore put on qualitative analysis methods instead of quantitative.

4.1. Methods

FEM analysis to determine stiffness ratios and eigenfrequency analysis are chosen as the methods to explore some of the properties of the alignment stages from the conceptual mechanism constructed in section 3.5. Stiffness ratios are a commonly used metric to determine how well a compliant mechanism performs. They can't be used in every situation however. The relation between rotational and translational stiffness can't be described by a ratio as these two types of stiffness do not have the same units. Eigenfrequencies can be used as a substitute in these cases. Eigenfrequencies and corresponding mode shapes give information about the compliance and stiffness ratios between constrained and unconstrained DoF. The information from stiffness ratios and eigenfrequencies is used to identify optimization opportunities such as moving flexures or altering their geometries. The effect of these optimizations is also illustrated with stiffness ratios and eigenfrequency analysis. A physical prototype in Ti6Al4V is used to explore assumptions about the manufacturing process.

4.2. Characterizing alignment stages

The performance of the centering alignment stage is described with a stiffness ratio between a horizontal and vertical translation. Comsol multiphysics is used to apply a load on the centering stage in the x, y and z axis. The displacements and loads are used to determine the stiffness in the Tx, Ty and Tz directions and determine the ratios between them. The results are included in table 6. An option to improve these ratios is investigated in section 4.3.

Eigenfrequency analysis is used to compare the relation between Tz-stiffness and Rx-stiffness of the focus alignment stage. The first two eigenmodes corresponding to these DoF of the focus alignment stage are shown in figure 24. The

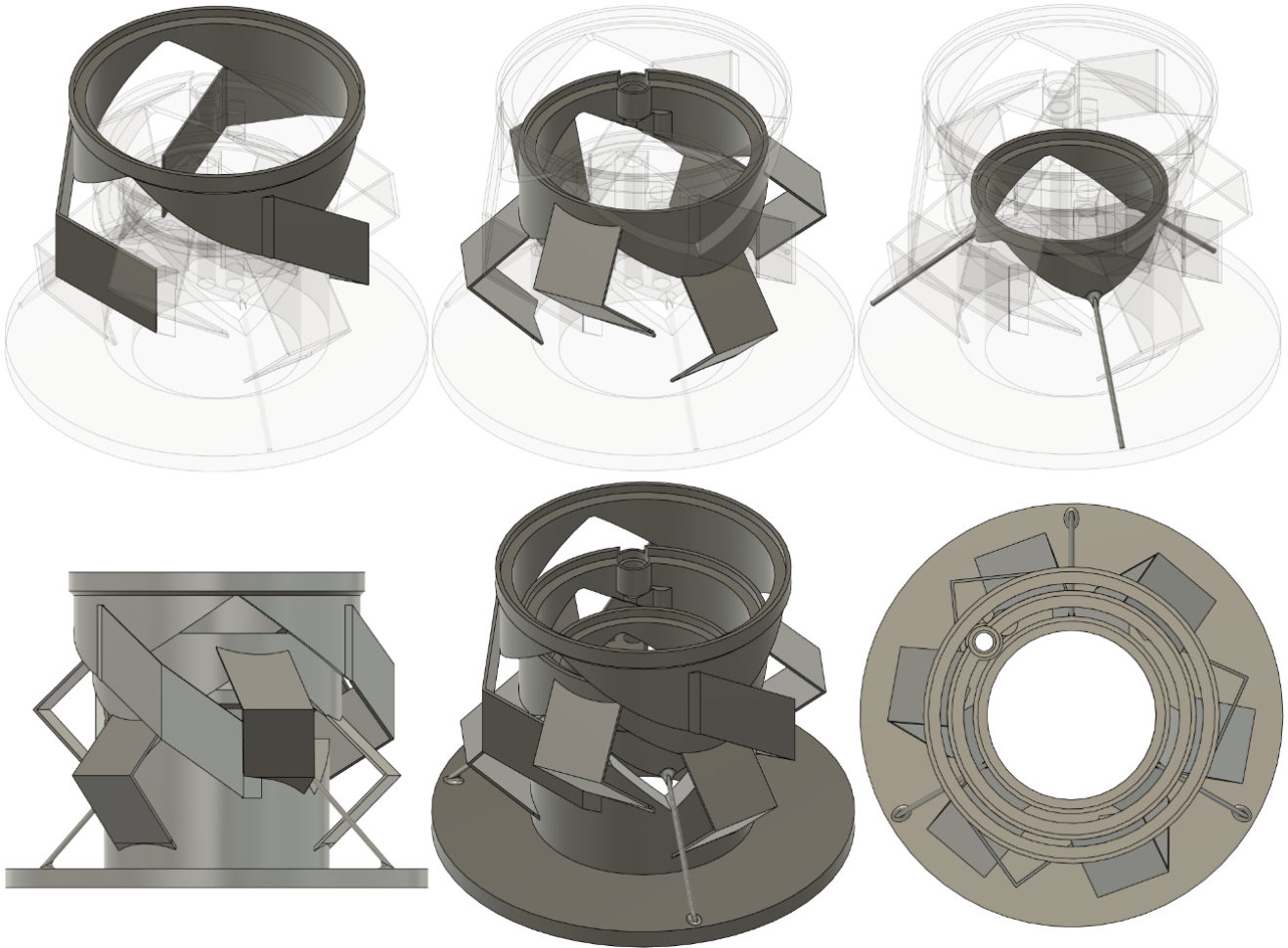


Figure 23: CAD model of the three alignment stages integrated into a concept design.

k_x	k_y	k_z	k_z/k_x	k_z/k_y
30kN/m	30kN/m	2.3MN/m	76.7	76.7

Table 6

Stiffness of the center alignment stage in Tx, Ty and Tz with stiffness ratios.

eigenfrequencies of these two eigenmodes are close together. Options to increase the difference between these eigenfrequencies are explored in section 4.3.

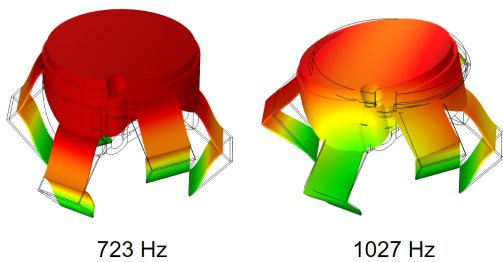


Figure 24: The first and second eigenfrequency and eigenmodes of the focus alignment mechanism, corresponding to the Tz and Rx DoF respectively.

The properties of the tip tilt alignment stage are also investigated using eigenfrequency analysis. The eigenfrequencies and mode shapes corresponding to Rx, Tx and Tz DoF are shown in figure 25. The mode shapes of Rx and Tx are separated by half an order of magnitude in eigenfrequency. The eigenfrequency of the Tz mode shape is higher than the Tx mode shape. Optimization options for the tip tilt alignment stage are explored in section 4.3.

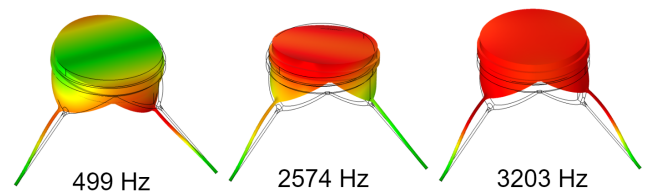


Figure 25: The 2nd, 4th and 6th eigenfrequencies and eigenmodes of the tip tilt alignment mechanism, corresponding to Rx, Tx and Tz DoF respectively.

4.3. Exploring improvements

Widening the folded leaf springs is explored as an option for improving the stiffness ratios of the centering stage. Dou-

k_x	k_y	k_z	k_z/k_x	k_z/k_y
67kN/m	67kN/m	8.2MN/m	122	122

Table 7

Stiffness of the center alignment stage where the width of the skewed folded leaf flexures has been increased from 7mm to 14mm in T_x , T_y and T_z with stiffness ratios.

bling the width of the folded leaf springs from 7mm to 14mm increases the force required for horizontal displacement but does not have a significant impact on maximum stress. The stiffness ratio between horizontal and vertical displacement has increased from 76.7 to 122, as shown in table 7.

Moving on to the focus stage, figure 24 shows that the difference between eigenfrequencies of its desired and undesired mode shapes is small. The eigenfrequencies of the undesired mode shape can be raised by increasing the distance between the two sets of three folded leaf flexures. The eigenfrequency of the first mode shape corresponding to the desired T_z movement can be decreased by rotating the upper set of folded leaf springs by 90 degrees. The in-plane stiffness contour of folded leaf springs is not symmetrical, as illustrated in figure 26 [7]. Rotating the folded leaf springs 90 degrees from their position in the focus stage decreases their stiffness in T_z , lowering the overall stage T_z -stiffness and the first eigenfrequency.

Rotating the upper folded leaf springs by 90 degrees increases both the vertical distance between the two sets of folded leaf springs and lowers the overall stiffness in the unconstrained DoF. Figure 27 shows that the eigenfrequency of the first mode shape has decreased due to the rotation of the folded leaf springs due to the lower stiffness in T_z . The 2nd eigenfrequency has increased significantly. Overall performance of the focusing stage is expected to increase sig-

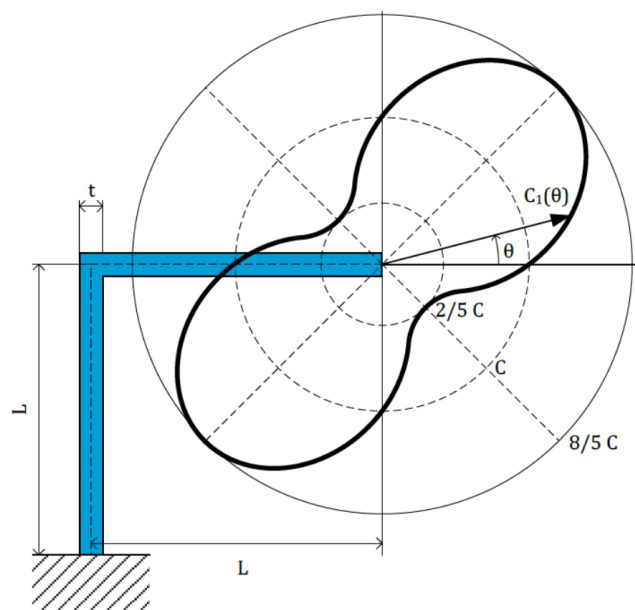


Figure 26: Angle dependent stiffness (C) contour for a folded leaf spring.

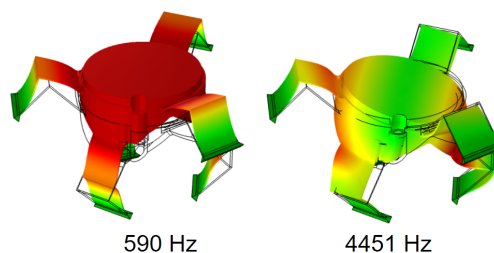


Figure 27: The eigenfrequencies and eigenmodes of the focus alignment mechanism corresponding to the T_z and R_x DoF.

nificantly.

Two options to optimize the behaviour of the tip tilt stage are explored. The overhang angle of the struts can be changed and the struts can be reinforced. Decreasing the overhang angle decreases stiffness in the T_z direction and increases stiffness in the xy -plane. Increasing the overhang angle has the opposite effect. The 4th mode shape corresponds to x -translation and the 6th mode shape corresponds to z -translation. Decreasing the strut angle is expected to move these eigenfrequencies closer together, increasing the 4th and decreasing the 6th. The difference between the 2nd and 4th eigenfrequency should increase. In figure 28 the 2nd, 4th and 6th eigenfrequencies are shown for the case where the strut angle has been decreased from 45 degrees to 40 degrees. As expected, the difference in eigenfrequency between the desired and undesired eigenmodes has increased. The difference in eigenfrequencies of the two undesired eigenmodes decreased from 0.6kHz to 0.1 kHz. This indicates that 40 degrees is close to the optimum strut overhang angle for this particular geometry of tip tilt stage if the goal is to maximise the difference between the 2nd and 4th eigenfrequency.

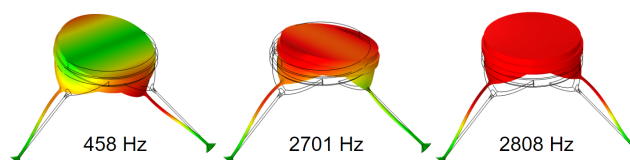


Figure 28: The 2nd, 4th and 6th eigenfrequencies and eigenmodes of the tip tilt alignment mechanism with a 40 degree overhang angle for the struts, corresponding to R_x , T_x and T_z DoF respectively.

The effect of reinforcing the struts on the eigenfrequencies and mode shapes is illustrated in figure 29. The struts are reinforced for 70% of their length. The increase in stiffness causes all eigenfrequencies to increase. The difference between the 2nd and 4th eigenfrequencies increases from approximately 2kHz to 2.5kHz, indicating an increase in stiffness ratios between constrained and unconstrained DoF. The magnitude of displacement for the 6th eigenmode has also visibly decreased compared to the magnitude of the same eigenmode for the non-reinforced tip tilt stage in figure 25.

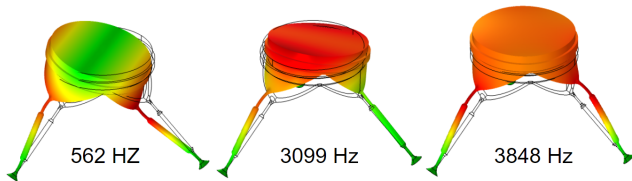


Figure 29: The 2nd, 4th and 6th eigenfrequencies and eigenmodes of the tip tilt alignment mechanism with reinforced struts, corresponding to Rx, Tx and Tz DoF respectively.

4.4. Prototype

A prototype is manufactured to explore some assumptions about the capabilities of the manufacturing process, as thin walled features, low overhang angles and converging geometries can result in printing defects. The alignment mechanism is designed to be manufactured in Ti6Al4V with the selective laser melting (SLM) process. The use of Ti6Al4V with SLM determines the specific design requirements on geometries. With this material overhang angles can be as low as 30 degrees. Minimum achievable values for wall thickness are 0.18mm (not gas tight) and 0.20 - 0.25mm (gas tight), and 0.18mm for pillars [2]. As walls and pillars grow taller, they become more fragile and prone to breaking either during or after printing. The minimum wall thickness in the prototype has been set to 0.3mm. Converging geometries can also result in printing defects. As two parts of a design start off as separate entities and eventually converge at a higher point, thermal effects can result in shrink lines. These shrink lines appear as small deformations and can impact part geometry. Converging geometries are mostly unavoidable in compliant mechanisms that are not extrusions of a 2D contour.

The produced prototype is depicted in figure 30. The dimensions of the vertical leaf flexure walls are measured at 0.45mm compared to 0.3mm as designed. The dimensions of the 45 degree angled leaf flexure walls are measured at 0.41mm compared to 0.3mm as designed. The dimensions of the strut flexures is measured at 0.71mm compared to 0.6mm as designed. This difference is attributed to surface roughness. There is visible porosity in the thin walled leaf flexures, with the 45 degree angled thin walled surfaces having slightly larger pores. The force to reach 0.5mm displacement on the centering stage is significantly lower compared to values derived from FEM analysis, indicating a possible decrease in effective thickness of the folded leaf flexures. There is no evidence of shrink lines in any of the converging points.

5. Conclusion

In this paper a novel design method for metal 3D printed compliant alignment mechanisms is developed and demonstrated. The method uses the desired constraints as an input and, through representing these constraints with strut configurations and substituting these struts with equivalent, printable geometries, is able to produce an overview of printable

building blocks. The constraints represented by strut configurations, substitution elements and an overview of printable building blocks for commonly used flexures are presented in three tables. The design method is presented as a flowchart and additionally explained by applying it step by step on a tip tilt example case. The design method is demonstrated by applying it towards a mechanism that aligns three optical elements in either tip tilt, focus or center. Concepts are developed for each stage using the design method. These concepts are then evaluated and integrated into a monolithic design. FEM analysis and a prototype in Ti6Al4V are used to explore some of the properties and manufacturability of this demonstration case. Options to improve performance of the alignment stages are proposed as a result of FEM analysis.

6. Recommendations

For future research it would be interesting to expand the scope beyond alignment mechanisms. Mounts for various optical components have yet to be considered. The limited capability to print geometries with low overhangs can make it difficult to print flexure-based mounts in some orientations. Printable alternatives that maintain symmetry of stiffness for multiple types of optical elements and orientations are needed to solve this problem. Another type of mounting for optical components that needs to be explored further is adhesive-based mounts. Adhesive Pockets and channels can be integrated into 3D printed mounts.

The development of a-thermal designs is another possible target for further research. Designs that minimize sensitivities to temperature changes are essential to maintain alignment of optical components within their tolerances. Asymmetric printable building blocks would be particularly interesting to develop into a-thermal designs. Other options for the management of thermals can be investigated such as integrated cooling channels and radiators.

The effects of the lack of support material during the printing of thin slender features such as flexures can be investigated. Warping effects may occur in these types of features which can affect material stress, with or without additional heat treatments, and influence the properties of alignment stages. Options such as small removable tabs can be investigated to replace traditional scaffold-based support material.

Not all strut configurations have been considered in the development of the printable building blocks presented in this paper. Some of these strut configurations may lead to more suitable printable building blocks for certain design requirements.

Additional substitution elements can be developed to increase the amount of printable building blocks that can be created for each strut configuration. The substitution elements presented in this paper can also be optimized for specific properties. This optimization can be done by varying width, length and thickness of the geometries, changing angles between parts of a substitution element and reinforcing compliant members. Topology optimization can also be



Figure 30: Alignment mechanism prototype produced in Ti6Al4V with SLM.

used to optimize existing substitution elements as well as generate new ones.

The scope of this thesis has been limited by only creating printable building blocks for a selection of constraint combinations and orientations. Future research could work on developing printable building blocks for constraint combinations that have not been considered in this thesis. It is also possible that not all printable building blocks have been created for the constraint combinations that have been considered in this thesis.

The constraint combinations and strut configurations from table 1, substitution elements from table 2 and printable building blocks from table 3 have all been developed for six DoF in the three cardinal directions. The only rotations that are considered are those that do not meaningfully change the free DoF of a strut configuration. The contents from table 1, 2 and 3 can be significantly expanded by also considering all other orientations of free and constrained DoF. A good starting point would be to consider all rotations of 45 degrees around the x- and y-axis for the 18 strut configurations. Rotations of 60 and 30 degrees could also still be useful to consider. Further divisions would probably result in strongly diminishing returns.

Methods of actuation could be developed for each considered orientation and integrated with the printable building blocks. Actuation devices like screws are often combined with actuation mechanisms that increase their resolution. These actuation mechanisms can also be developed for each considered orientation and integrated with printable building blocks. Locking methods would also be useful to integrate in this same manner.

Additional printable building blocks can be developed by making strategic use of the build plate removal process. After a part is printed it is released from the build plate with, for example, spark erosion. This machining operation can be used to separate parts of a mechanism from each other after printing. This method can be used to fold compliant mechanisms in on themselves, reducing their height. Printable

building blocks can also be developed to make strategic use of support material. Support material can support a moving body and be removed after printing to release the moving body. Like the method that relies on the build plate removal process, using support material in this manner can be used to make more compact printable building blocks.

It would be very interesting to apply the design method to real design cases. Alternatives to already existing mechanisms can be created to compare performance, manufacturing costs, assembly/post-processing time and development time. Applying the design method to a new design case would also provide valuable information on its efficacy.

References

- [1] 3D Systems, 2020. LaserForm® Ti Gr5 (A) 5, 1–2.
- [2] 3D Systems, I., 2018. Design Guide - Direct Metal Printing , 35.
- [3] Boyer, R., Welsch, G., Collings, E., 1994a. Materials Properties Handbook - Titanium Alloys 32.10 Thermal Properties. ASM International. URL: <https://app.knovel.com/hotlink/khtml/id:kt007TGRD2/materials-properties/ti-6al-4v-thermal-properties>.
- [4] Boyer, R., Welsch, G., Collings, E., 1994b. Materials Properties Handbook - Titanium Alloys 32.11 Design Mechanical Properties. ASM International. URL: <https://app.knovel.com/hotlink/khtml/id:kt007TGRE1/materials-properties/design-mechanical-properties>.
- [5] Gibson, I., Rosen, D., Stucker, B., 2015. Directed Energy Deposition Processes. In: Additive Manufacturing Technologies.
- [6] Hopkins, J.B., Culpepper, M., 2007. Design of Parallel Flexure Systems via Freedom and Constraint Topologies (FACT). Department of Mechanical Engineering MSc, 393.
- [7] JPE-innovations, 10-10-2021. Precision point 3 parallel tangential folded leaf springs. URL: <https://www.jpe-innovations.com/precision-point/3-parallel-tangential-folded-leaf-springs/>.
- [8] Katie Schwertz, J.B., 2012. Field Guide to Optomechanical Design and Analysis. SPIE Press. SPIE Field Guide Vol. FG26, p. 29.
- [9] van der Lee, N., Kappelhof, J.P., Hamelinck, R., 2003. Flexure-based alignment mechanisms: design, development, and application. Optomechanics 2003 5176, 94. doi:10.1117/12.509135.
- [10] Lobontiu, N., 2002. Compliant Mechanisms: Design of Flexure Hinges (1st ed.). CRC Press.
- [11] Schott Inc., Schott Advanced Optics, 2004. TIE-32 : Thermal loads on optical glass .

- [12] Smith, S., 2000. Flexures: Elements of Elastic Mechanisms (1st ed.). CRC Press.
- [13] Sommer, D., Götzendorfer, B., Esen, C., Hellmann, R., 2021. Design Rules for Hybrid Additive Manufacturing Combining Selective Laser Melting and Micromilling , 1–23.

7

Conclusion and recommendations

7.1. Conclusion

The introduction of this thesis discusses the current situation of designing compliant alignment mechanisms for metal 3D printing. Improving and expanding the set of tools that designers can use to solve the design challenges associated with these types of mechanisms is set as a long term goal. This set of tools is envisioned as a design method with building blocks, guidelines and strategies. The goal of this thesis is to generate a start towards achieving this goal. The requirements for this start are a set of printable building blocks, a system to order these elements and a method to use them to construct concepts for any type of alignment.

A solution to fulfill these research goals is presented in chapter two. The concept of printable building blocks has been split into three parts; constraint combinations with strut configurations, printable building blocks and substitution elements. The strut configurations represent the constraints on a moving body in a physical, visual manner. The printable building blocks can be used to construct alignment mechanism concepts. The conversion between the strut configurations and printable building blocks is done through the use of substitution elements.

The strut configurations for each DoF combination are presented in table 1. The strut configurations that correspond to the DoFs of commonly used flexure elements are converted to printable building blocks using the substitution elements in table 2. The resulting printable building blocks are presented in table 3. Using the tables to construct concepts is done with a design method described in a flowchart, shown in figure 4.

The method is demonstrated by using it to develop a compact three stage alignment mechanism. Some of the properties of this mechanism are explored with FEM analysis. Stiffness ratios and eigenfrequencies are used to describe some characteristics of each stage. Several options to improve these characteristics are then proposed. The effect of these improvements are compared to the original design. Additionally, some of the assumptions about the manufacturing process are investigated using a prototype manufactured in Ti6Al4V.

There are some of aspects in which the method could be expanded. First of all, not all possible strut configurations are presented in table 1. This decision was made to keep the overview reasonably compact and to limit the scope of this thesis. Not all strut configurations are equally useful and preference goes towards simpler strut configurations because their lower strut count results in simpler printable building blocks and therefore simpler mechanism concepts. There could be specific situations in which one of the omitted strut configurations would have resulted in a better selection of concepts to fulfill certain design requirements. Following the design method may not always result in the most optimal solution possible for each set of requirements. The method should be treated as an additional design tool and not as a replacement for other design methods.

Secondly, the scope of this thesis has been limited by only considering three orientations of the constraint combinations presented in table 1. In reality the constraint orientations are not limited to three cardinal directions but exists in a continuum. This means that some solutions, that may better fit certain design requirements, are not considered.

Thirdly, the method assumes that the primary limitation on printable geometries is the overhang angle. As metal 3D printing processes improve this assumption may no longer be accurate.

7.2. Recommendations

For future research it would be interesting to expand the scope beyond alignment mechanisms. Mounts for various optical components have yet to be considered. Flexures are used in many alignment mechanisms to mount optical components. Just like the flexures used for the movement of the alignment mechanism, those used for mounting purposes cannot always simply be printed in the same orientation as they would be in conventionally manufactured mechanisms. The limited capability to print geometries with low overhangs can make it difficult to print flexure-based mounts in some orientations. Printable alternatives that maintain symmetry of stiffness for multiple types of optical elements and orientations are needed to solve this problem. Another type of mounting for optical components that needs to be explored further is adhesive-based mounts. Pockets and channels for adhesives can be integrated into 3D printed mounts.

The development of a-thermal designs is another possible target for further research. Thermal effects can have considerable impacts on the accuracy and stability of the alignment of optical components. Designs that minimize sensitivities to temperature changes are essential to maintain alignment of optical components within their tolerances, especially in environments where the temperature is varying and cannot be controlled. Asymmetric printable building blocks would be particularly interesting to develop into a-thermal designs, as the lessons learned from those cases may be applicable to all printable building blocks. Other options for the management of thermals can be investigated. Designs with integrated cooling channels and radiators could help mitigate thermal effects in situations where a-thermal designs are not feasible or sufficient to maintain alignment tolerances.

The effects of the lack of support material during the printing of thin slender features such as flexures can be investigated. Warping effects may occur in these types of features which can affect material stress, with or without additional heat treatments, and influence the properties of alignment stages. Guidelines can be compiled for in which situations support material should be included, which could include features that already have self-supporting overhang angles. Options such as small removable tabs can be investigated to replace traditional scaffold-based support material to reduce post-processing time.

As mentioned before, not all strut configurations have been considered in the development of the printable building blocks presented in this thesis. Some of these strut configurations may lead to more suitable printable building blocks for certain design requirements. Expanding the set of strut configurations and developing printable building blocks using the design method could lead to interesting results.

The substitution elements presented in table 2 are most likely not the only substitution elements possible. Developing additional substitution elements increases the amount of printable building blocks that can be created for each strut configuration. The substitution elements presented in this thesis can also be optimized for specific properties such as higher stiffness ratios between certain directions, minimizing stress concentrations, reducing mass, minimizing volume claim and providing additional area to build subsequent layers from. This optimization can be done by varying width, length and thickness of the geometries, changing angles between parts of a substitution element and reinforcing compliant members. Topology optimization can also be used to optimize existing substitution elements as well as generate new ones. Different constraints on these topology optimizations could result in a much larger collection of substitution elements, significantly expanding the amount of printable building blocks that can be constructed.

The overview of printable building blocks in table 3, together with the printable building blocks developed for the three alignment stages of the demonstration mechanism, is presented in appendix A. The printable building blocks in this appendix are sorted by constraint combination and strut representation. As can be seen in this appendix, there are a number of empty rows. The scope of this thesis has been limited by only creating printable building blocks for a selection of constraint combinations and orientations. Future research could work on developing printable building blocks for constraint combinations that have not been considered in this thesis. It is also possible that not all printable building blocks have been created for the constraint combinations that have been considered in this thesis. Additional research can be done to complete the printable building block overview in appendix A for these constraint combinations as well.

The constraint combinations and strut configurations from table 1, substitution elements from table 2 and printable building blocks from table 3 have all been developed for six DoF in the three cardinal directions. The only rotations that are considered are those that do not meaningfully change the free DoF of a strut configuration. For example, a linear guide with Tx can be rotated by any amount around the x-axis and still remain a linear guide in Tx. The scope of the contents from table 1, 2 and 3 can be significantly expanded by also considering all other orientations of free and constrained DoF. This significantly expands the options to combine multiple alignment mechanisms in one monolithic print. Currently, one alignment mechanism with two focus stages at a right angle to each other, with one being in Tz and one in Tx, would require very different

printable building blocks for each of these alignment stages. If 45 degree rotations are also considered, the two focus mechanisms could both be printed at 45 degrees and be identical. A good starting point would therefore be to consider all rotations of 45 degrees around the x- and y-axis for the 18 strut configurations. Rotations of 60 and 30 degrees could also still be useful to consider. Further divisions would probably result in strongly diminishing returns.

Methods of actuation could be developed for each considered orientation and integrated with the printable building blocks. These could be mounting points for push-pull pairs, push push pairs, differential screws or any other type of actuation. Actuation devices like screws are often combined with actuation mechanisms that increase their resolution. These actuation mechanisms can also be developed for each considered orientation and integrated with printable building blocks. Locking methods would also be useful to integrate in this same manner.

Additional printable building blocks can be developed by making strategic use of the build plate removal process. After a part is printed it is released from the build plate with, for example, spark erosion. This machining operation can be used to separate parts of a mechanism from each other after printing. This method can be used to fold compliant mechanisms in on themselves, reducing their height. This makes the mechanism both more compact and cheaper to manufacture. The printable building blocks presented in table 3 are designed to not rely on this release from the build plate to become functional. Additional printable building blocks can be developed to make use of this method.

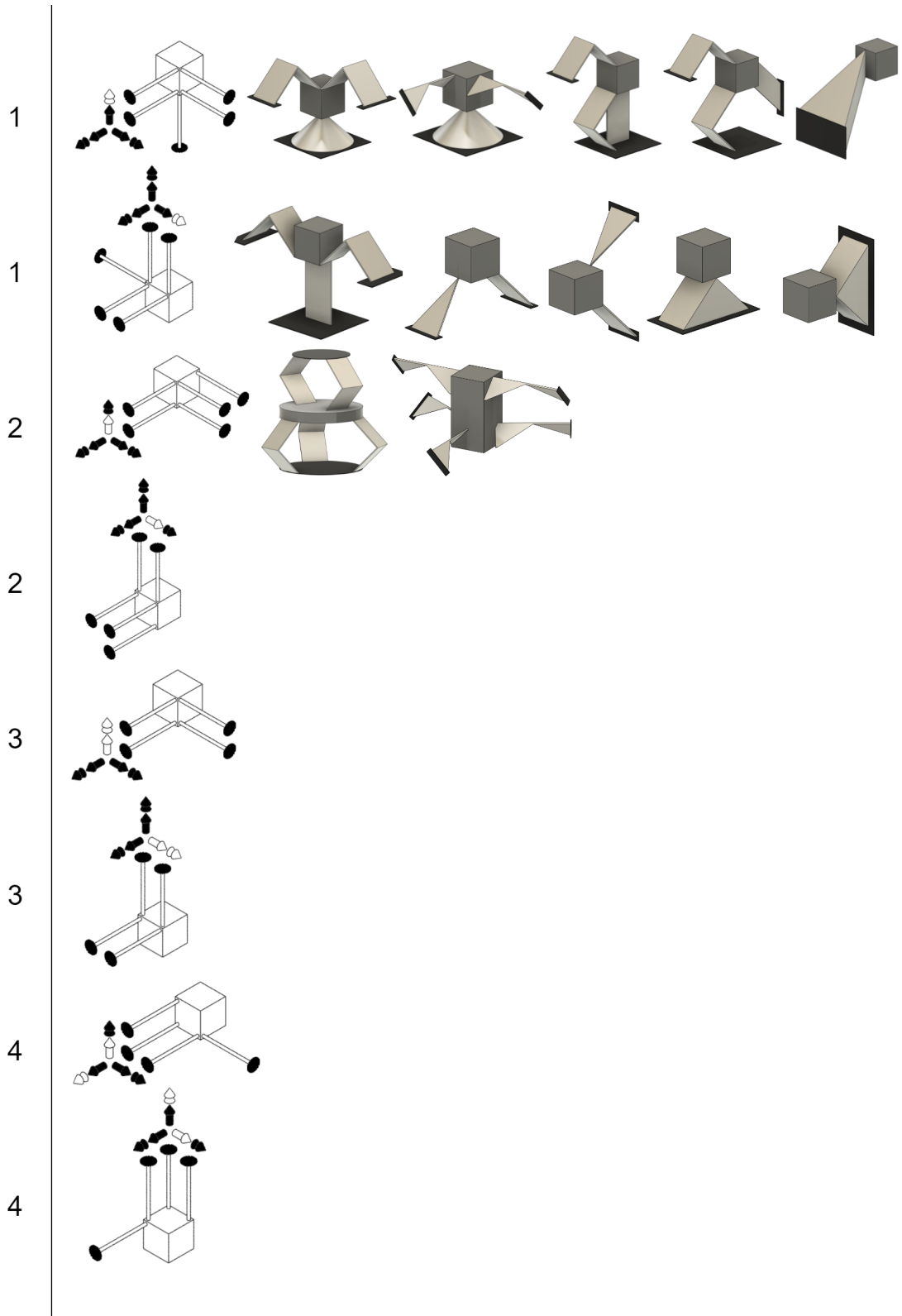
Printable building blocks can also be developed to make strategic use of support material. Using support material to print thin walled flexures with low overhang angles affects the thickness and surface quality of these flexures. Only using support for non-compliant moving bodies does not have these same downsides. Support material can support a moving body and be removed after printing to release the moving body. Like the method that relies on the build plate removal process, using support material in this manner can be used to make more compact printable building blocks.

It would be very interesting to apply the design method to real design cases. Alternatives to already existing mechanisms can be created to compare performance, manufacturing costs, assembly/post-processing time and development time. Applying the design method to a new design case would also provide valuable information on its efficacy.

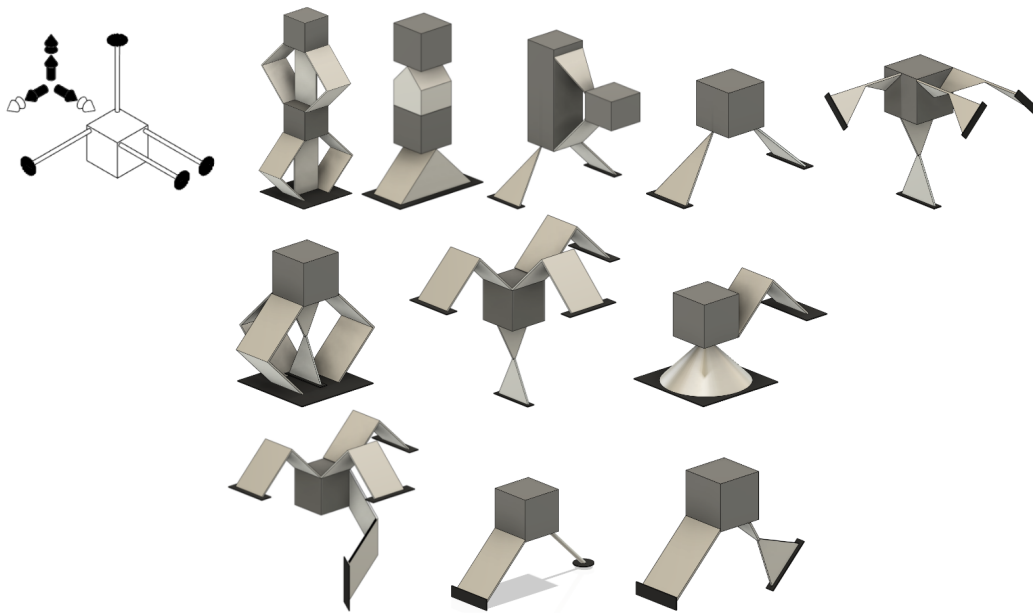
A

Appendix

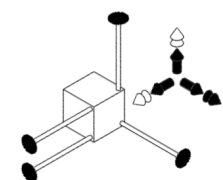
This appendix contains all printable building blocks created during this thesis. The printable building blocks are sorted by their constraint combination and strut representation numbers. These constraint combination and strut representation numbers can be found in table 1. Building blocks with reflectional symmetry in the vertical plane have only been included once to prevent duplicate information.



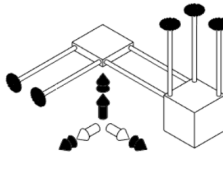
5



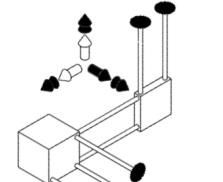
5



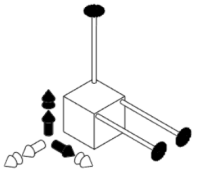
6

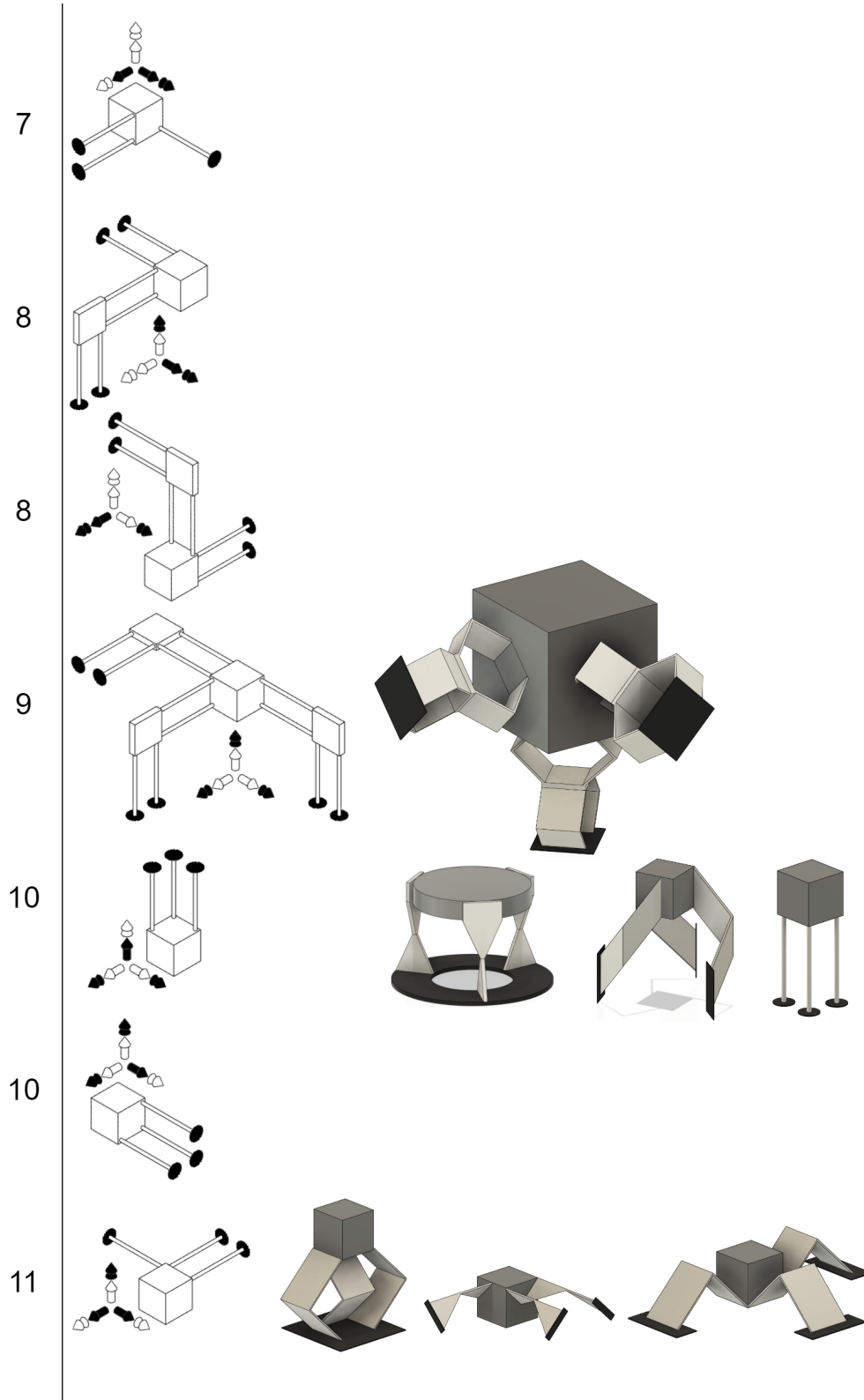


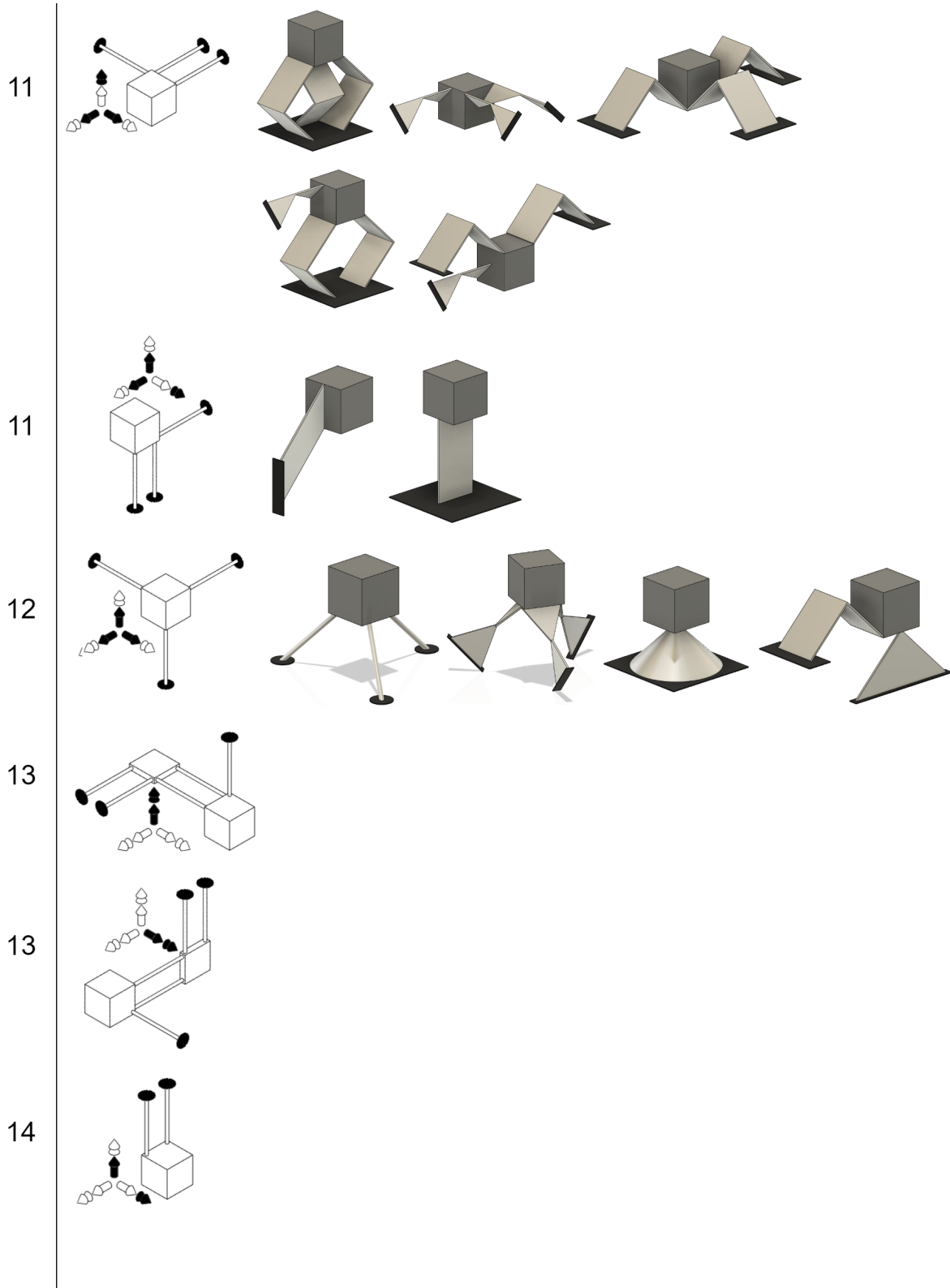
6

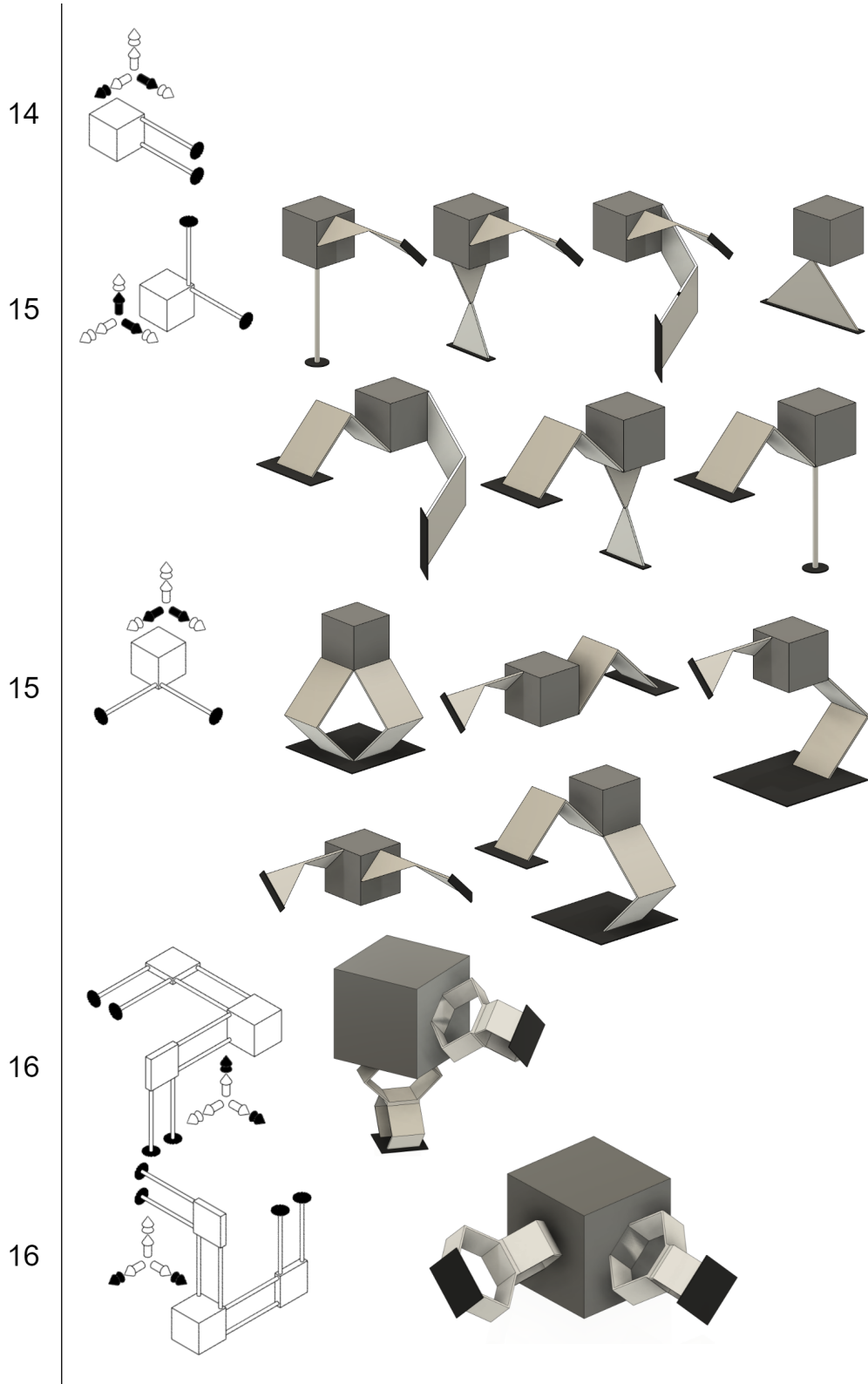


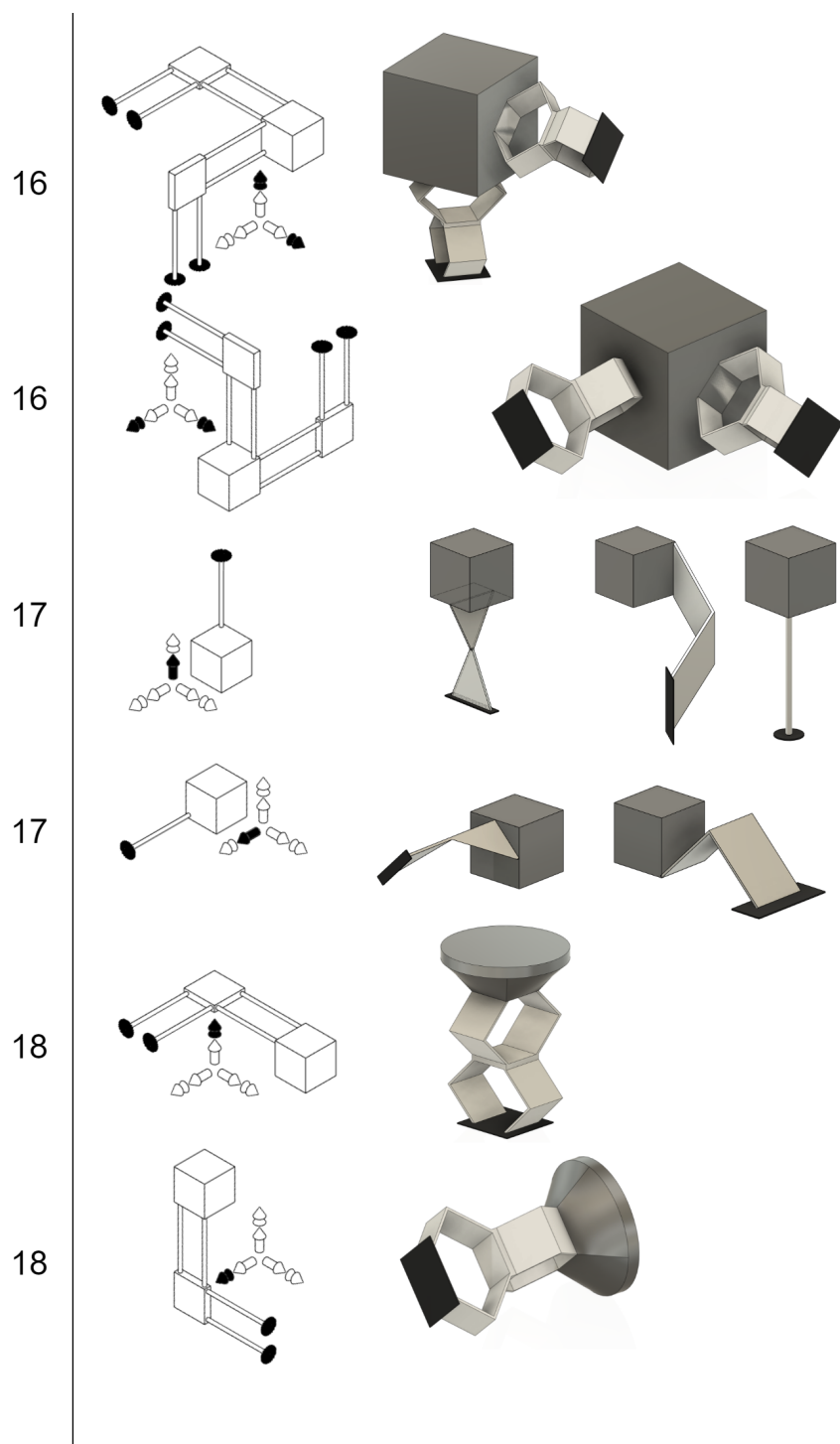
7











Bibliography

- [1] Inc. 3D Systems. Design Guide - Direct Metal Printing. page 35, 2018.
- [2] R. Boyer, G. Welsch, and E.W. Collings. *Materials Properties Handbook - Titanium Alloys 32.11 Design Mechanical Properties*. ASM International, 1994. ISBN 978-0-87170-481-8. URL <https://app.knovel.com/hotlink/khtml/id:kt007TGRE1/materials-properties/design-mechanical-properties>.
- [3] R. Boyer, G. Welsch, and E.W. Collings. *Materials Properties Handbook - Titanium Alloys 32.10 Thermal Properties*. ASM International, 1994. ISBN 978-0-87170-481-8. URL <https://app.knovel.com/hotlink/khtml/id:kt007TGRD2/materials-properties/ti-6al-4v-thermal-properties>.
- [4] F. Calignano. Design optimization of supports for overhanging structures in aluminum and titanium alloys by selective laser melting. *Materials and Design*, 64:203–213, 2014. ISSN 18734197. doi: 10.1016/j.matdes.2014.07.043. URL <http://dx.doi.org/10.1016/j.matdes.2014.07.043>.
- [5] Milan Dana, Ivana Zetkova, and Pavel Hanzl. Need for support structures depending on overhang size. *MM Science Journal*, 2016(DECEMBER):1597–1601, 2016. ISSN 18050476. doi: 10.17973/MMSJ.2016_12_2016192.
- [6] Ian Gibson, David Rosen, and Brent Stucker. *Directed Energy Deposition Processes. In: Additive Manufacturing Technologies*. 2015. ISBN 9781493921126.
- [7] Jonathan B Hopkins and Martin Culpepper. Design of Parallel Flexure Systems via Freedom and Constraint Topologies (FACT). *Department of Mechanical Engineering*, MSc:393, 2007.
- [8] James Burge Katie Schwertz. *Field Guide to Optomechanical Design and Analysis*, page 29. SPIE Field Guide Vol. FG26. SPIE Press, 2012. ISBN 0819491616; 9780819491619.
- [9] N. Lobontiu. *Compliant Mechanisms: Design of Flexure Hinges (1st ed.)*. CRC Press, 2002. ISBN 9780429121654.
- [10] Schott Inc. and Schott Advanced Optics. TIE-32 : Thermal loads on optical glass. 2004.
- [11] S.T. Smith. *Flexures: Elements of Elastic Mechanisms (1st ed.)*. CRC Press, 2000. ISBN 9781482282962.
- [12] Daniel Thomas, Hons Computer, and Aided Product. The Development of Design Rules for Selective Laser Melting The Development of Design Rules for Selective Laser Melting. 2010.
- [13] Di Wang, Shuzhen Mai, Dongming Xiao, and Yongqiang Yang. Surface quality of the curved overhanging structure manufactured from 316-L stainless steel by SLM. *International Journal of Advanced Manufacturing Technology*, 86(1-4):781–792, 2016. ISSN 14333015. doi: 10.1007/s00170-015-8216-6.